119

BioRadiations

A Resource for Life Science Research

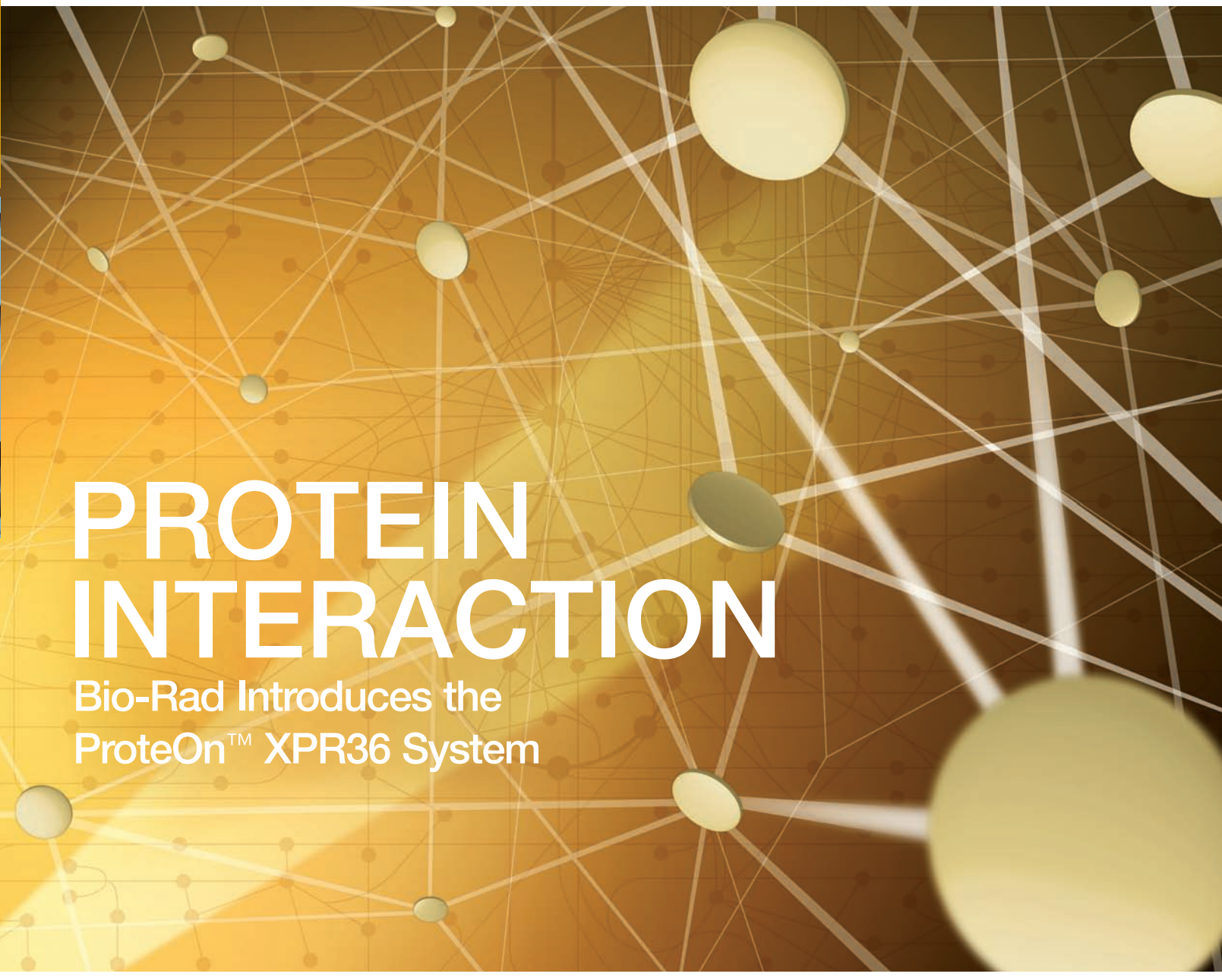

PROTEIN INTERACTION

Bio-Rad Introduces the ProteOn™ XPR36 System

In this issue:

Analysis of Multiple Protein Interactions
Considerations for Multiplex PCR Assays
Microarray Imaging With a Benchtop Imager
Purification Methods for Tagged Proteins

BIO-RAD

Under the hood, you'll find the same engine.

Now that MJ Research is part of Bio-Rad, the color of the MJ family of instruments is changing. But our commitment to innovation and service remains.

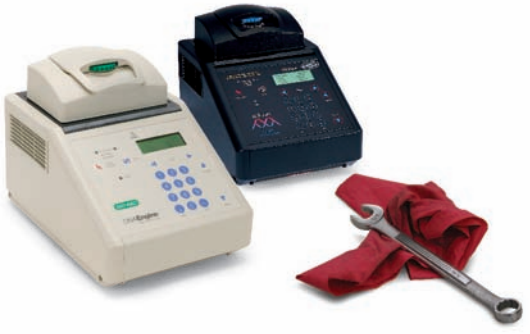

Bio-Rad is excited to offer the most comprehensive range of thermal cyclers and real-time PCR systems available, with one just right for you.

For over 50 years, Bio-Rad has delivered innovative and effective amplification products to life science professionals around the world. Our solutions are designed by scientists, for scientists.

For information on the complete suite of Bio-Rad amplification products, visit us on the Web at **www.bio-rad.com/amplification/**

Visit us on the Web at **discover.bio-rad.com**
Call toll free at 1-800-4BIORAD (1-800-424-6723);
outside the US, contact your local sales office.

BIO-RAD

BIO-RAD SUBSIDIARY
TELEPHONE NUMBERS

Australia 61-2-9914-2800
Austria 43-1-877-89-01
Belgium 32-9-385-55-11
Brazil 55-21-3237-9400
Canada 905-712-2771
China 86-21-6426-0808
Czech Republic 420-241-430-532
Denmark 45-44-52-10-00
Finland 358-9-804-22-00
France 33-1-47-95-69-65
Germany 49-89-318-84-0
Hong Kong 852-2-789-3300
Hungary 36-1-455-8800
India 91-124-402-9300
Israel 03-963-6050
Italy 39-06-5295892
Japan 81-3-5811-6270
Korea 82-2-3473-4460
Latin America 00-1-305-894-5950
Mexico 55-52-00-05-20
The Netherlands 31-318-540666
New Zealand 64-9-415-2280
Norway 47-23-38-41-30
Poland 48-22-331-99-99
Portugal 351-21-472-7700
Russia 7-095-721-14-04
Singapore 65-6415-3188
South Africa 27-861-246-723
Spain 34-91-590-5200
Sweden 46-8-555-12700
Switzerland 41-61-717-9555
Taiwan 88-62-2578-7189
Thailand 662-651-8311
United Kingdom 44-20-8328-2000
USA Toll free 1-800-4BIORAD
(1-800-424-6723)

discover.bio-rad.com

On the cover:
Conceptual illustration by
Chris Crutchfield

BioRadiations magazine is published by
Bio-Rad Laboratories, Inc.
2000 Alfred Nobel Drive
Hercules, CA 94547 USA

BioRadiations

issue 119, 2006

TO OUR READERS

Surface plasmon resonance (SPR) biosensors are proving valuable for high-resolution kinetic analyses of the fundamental interactions of proteins with other proteins and with other biomolecules, such as oligonucleotides, lipids, carbohydrates, and viruses. Tools to study such interactions have enormous potential to better characterize the role of expressed proteins in a wide variety of research fields. Bio-Rad's ProteOn™ XPR36 protein interaction array system is an SPR biosensor that combines state-of-the-art microfluidics, advanced optics, and an innovative sensor chip design to measure up to 36 individual biomolecular interactions in real time. In our cover story, both the system and its underlying technology are highlighted.

COVER STORY

16 **Analyzing Protein Interactions With the ProteOn XPR36 Protein Interaction Array System**
M Bartholdi, Bio-Rad Laboratories, Inc., Hercules, CA USA

DEPARTMENTS

2 **What's New**

6 **New Literature**

DIMENSIONS

7 **Convenient Multiplex PCR Assays With iQ™ Multiplex Powermix**
L Jordan and N Aslam, Bio-Rad Laboratories, Inc., Hercules, CA USA

TECHNICAL REPORTS

10 **Monitoring the Expression, Purification, and Processing of GST-Tagged Proteins Using the Experion™ Automated Electrophoresis System**
X He and W Strong, Bio-Rad Laboratories, Inc., Hercules, CA USA

13 **Enriching Basic and Acidic Rodent Brain Proteins With Ion Exchange Spin Columns for Two-Dimensional Gel Electrophoresis**
N Liu, R Gomez, S Freeby, K Academia, T Wehr, Y Yan, J Hey, and A Paulus, Bio-Rad Laboratories, Inc., Hercules, CA USA

22 **Analysis of Multiple Protein-Protein Interactions Using the ProteOn XPR36 Protein Interaction Array System**
V Bronner,[1] T Bravman,[1] A Notcovich,[1] D Reichmann,[2] G Schreiber,[2] and K Lavie[1], [1]Bio-Rad Laboratories, Inc., Technion, Haifa, Israel, [2]Weizmann Institute of Science, Rehovot, Israel

25 **Rapid and Detailed Analysis of Multiple Antigen-Antibody Pairs Using the ProteOn XPR36 Protein Interaction Array System**
V Bronner, T Bravman, and K Lavie, Bio-Rad Laboratories, Inc., Technion, Haifa, Israel

28 **Using the Molecular Imager® PharosFX™ System to Image Arrays Printed With the BioOdyssey™ Calligrapher™ MiniArrayer**
C Karlak, K McDonald, T Redila-Flores, and L Ugozzoli, Bio-Rad Laboratories, Inc., Hercules, CA USA

30 **Automated Three-Dimensional Purification Method for Histidine-Tagged Proteins Using the BioLogic DuoFlow Maximizer™ Chromatography System**
F-F Wu and R Provost, Bio-Rad Laboratories, Inc., Hercules, CA USA

Legal Notices — See page 6.

siLentMer™ Validated and Nonvalidated Dicer-Substrate siRNA Duplexes

Bio-Rad has partnered with Integrated DNA Technologies (IDT) to develop ready-to-transfect 27-mer Dicer-substrate siRNA duplexes, and now offers a collection of both validated and nonvalidated siLentMer siRNA duplexes. To simplify RNAi workflow, selected duplexes are available as siLentMer siRNA transfection kits, providing simple siRNA delivery and validated controls (see opposite page).

Dicer-Substrate siRNA — The Next Generation of siRNA Technology

It was once believed that only 21–23 nt double-stranded siRNAs would activate the RNAi pathway without triggering an interferon response (Elbashir et al. 2001). However, studies performed by the City of Hope and IDT demonstrate that 27 nt siRNA duplexes effectively activate the RNAi pathway at an earlier step than classical 21-mers without activating an interferon response (Kim et al. 2005). Their data suggest that these 27 nt duplexes are processed by the RNase III family member Dicer, and demonstrate that the 27-mer siRNAs are often more effective at silencing than a corresponding 21-mer.

Advantages of siLentMer Dicer-Substrate siRNA Duplexes

- Both validated and nonvalidated siRNA duplexes available
- Generally more efficient at lower concentrations (≤5 nM siRNA) than 21-mer siRNAs
- Homology analyzed for knockdown specificity using advanced bioinformatics to reduce the potential for off-target effects
- Proven 27-mer design algorithm results in siRNA with a high likelihood of effective silencing
- HPLC-purified for consistent and reliable results
- Ready-made designs for a variety of targets

The siLentMer validated siRNA duplexes are functionally tested to guarantee >85% reduction in mRNA expression. Two different siRNA duplexes are offered per target to allow confirmation of results. A variety of siLentMer nonvalidated siRNA duplexes are available, with a choice of four different duplexes per target.

To see data, view a list of currently available targets, and learn more about these siRNA duplexes, go to **www.bio-rad.com/RNAi/**. Be sure to check the site frequently for additional validated targets and new features describing advances in RNAi technology.

Ordering Information

Catalog #	Description
Varies	siLentMer Validated Dicer-Substrate siRNA Duplexes, 2 nmol, designed with proven criteria and functionally tested for >85% silencing
Varies	siLentMer Nonvalidated Dicer-Substrate siRNA Duplexes, 2 nmol, designed with proven criteria

References

Elbashir SM et al., Duplexes of 21-nucleotide RNAs mediate RNA interference in cultured mammalian cells, Nature 411, 494–498 (2001)

Kim DH et al., Synthetic dsRNA Dicer substrates enhance RNAi potency and efficacy, Nat Biotechnol 23, 222–226 (2005)

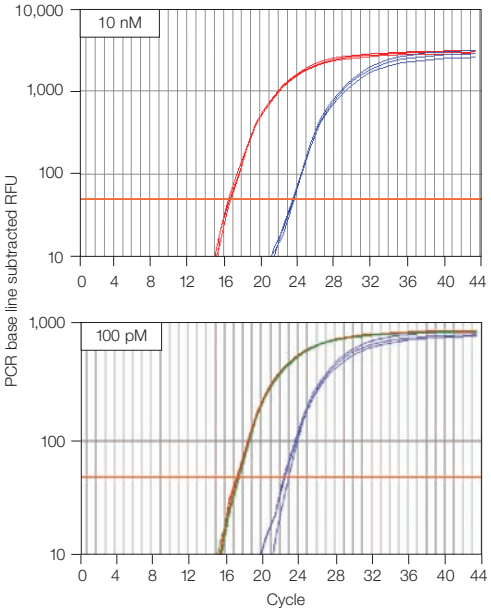

siLentMer siRNA duplexes mediate effective knockdown with low concentrations of siRNA. HeLa cells were transfected with 10 nM or 100 pM anti-GAPDH siRNA in a 12-well plate using 0.6 µl siLentFect lipid reagent per well. At 48 hr posttransfection, total RNA was extracted and RT-qPCR performed using the iScript™ cDNA synthesis kit and the iCycler iQ® real-time detection system. In both cases, the level of GAPDH transcript (■) was reduced by >95% relative to a nonsilencing control (■).

siLentMer™ siRNA Transfection Kits

To simplify RNAi experiments and optimize transfections using valid positive and negative controls, siLentMer siRNA transfection kits are now available with siLentFect™ lipid reagent and with validated and fluorescently labeled siLentMer siRNA duplexes. These kits include protocols and reagents to assist you in establishing appropriate controls and effective silencing conditions for your cell line. Key components of the siLentMer siRNA transfection kits include:

- siLentMer validated Dicer-substrate siRNA duplexes — a convenient, ready-to-use positive control for RNAi experiments
- Fluorescently labeled siLentMer nonsilencing siRNA — a useful control to visually establish effective delivery conditions and help monitor transfection efficiency
- siLentFect lipid reagent — an effective mediator of siRNA delivery for a broad range of cell lines, using either 21-mer siRNA or 27-mer Dicer-substrate siRNA

siLentMer Delivery Optimization Kit

This kit comes with a fluorescently labeled (CAL Fluor Red 610) nonsilencing 27-mer siRNA, to assess and establish optimal delivery conditions for any cell line. This delivery optimization kit contains reagents for up to 150 transfections in 24-well plates.

siLentMer Starter Kits

These cost-effective kits allow you to optimize delivery conditions and establish reliable positive and negative controls for your cell line. They include sufficient reagents for up to 150 transfections in 24-well plates.

siLentMer Total Control Kits

These kits include several validated 27-mer Dicer-substrate siRNA duplexes targeting common reference genes as well as GFP or luciferase siRNAs for cotransfection experiments involving plasmid-based reporter genes. These kits come with ample reagents, controls, and buffers for up to 300 transfections in 24-well plates, allowing you to run needed controls while you evaluate silencing of a target gene.

Ordering Information

Catalog #	Description
siLentMer Delivery Optimization Kit	
174-9950	siLentMer Delivery Optimization Kit, includes 1.0 nmol fluorescently labeled siLentMer nonsilencing siRNA, 0.2 ml siLentFect lipid reagent, 1.0 ml siLentMer siRNA resuspension buffer
siLentMer Starter Kits	
174-9960	siLentMer Starter Kit for Human GAPDH, includes 0.5 nmol siLentMer validated human GAPDH siRNA, 0.5 nmol siLentMer nonsilencing siRNA, 0.2 ml siLentFect lipid reagent, 1.0 ml siLentMer siRNA resuspension buffer
174-9961	siLentMer Starter Kit for GFP, includes 0.5 nmol siLentMer validated GFP siRNA, 0.5 nmol siLentMer nonsilencing siRNA, 0.2 ml siLentFect lipid reagent, 1.0 ml siLentMer siRNA resuspension buffer
siLentMer Total Control Kits*	
174-9970	siLentMer Total Control Kit for Human GAPDH
174-9971	siLentMer Total Control Kit for Human HPRT
174-9972	siLentMer Total Control Kit for Human Lamin A/C
174-9973	siLentMer Total Control Kit for Human Cyclophilin
174-9974	siLentMer Total Control Kit for Human β-Actin
174-9975	siLentMer Total Control Kit for Human β-Tubulin
174-9976	siLentMer Total Control Kit for GFP
174-9977	siLentMer Total Control Kit for Luciferase

* All total control kits include 1.0 nmol siLentMer validated siRNA (positive control), 1.0 nmol fluorescently labeled siLentMer nonsilencing siRNA (control for delivery), 1.0 nmol unlabeled siLentMer nonsilencing siRNA (negative control for silencing), 0.5 ml siLentFect lipid reagent, 1.0 ml siLentMer siRNA resuspension buffer.

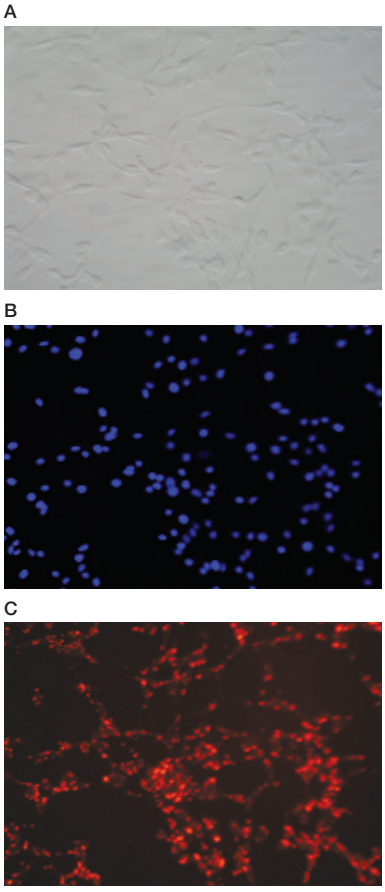

NIH-3T3 cells transfected with CAL Fluor Red 610 dye-labeled 27-mer siRNA using siLentFect lipid reagent. At 24 hr posttransfection, cells were fixed and stained with Hoechst dye. Cells were imaged using brightfield optics (**A**) and then analyzed by fluorescent microscopy to detect nuclear staining (**B**) and siRNA intake (**C**).

iQ™5 Optical System Software Security Edition

Added Security for Real-Time PCR Analysis

The iQ5 system combines excellent thermal performance from the iCycler® thermal cycler, sensitive real-time PCR detection from the iQ5 optics module, and comprehensive data analysis and reporting tools from the iQ5 optical system software. Now you can integrate the power of the iQ5 real-time PCR detection system with your laboratory's good laboratory practice (GLP) standards for data collection and data analysis with the new Security Edition of the iQ5 optical system software. This software upgrade is designed for routine use by scientists who operate in regulated environments that require consistent tracking of data collection methods.

This value-added security edition of the iQ5 software offers several major functions and features not available in the standard version, including:

- Embedded tools for compliance with US FDA 21 CFR Part 11 regulations, including electronic signature and added traceability features
- Advanced gene expression analysis methods that allow analysis of results from up to 10 data files simultaneously
- Enhanced reporting tools for customizing the secure presentation of assay results

Regardless of your PCR application, the iQ5 real-time PCR detection system offers value and flexibility. To learn more about the iQ5 optical system software Security Edition, or the complete iQ5 multicolor real-time PCR detection system, visit us on the Web at **www.bio-rad.com/realtime/**

Ordering Information

Catalog #	Description
170-9753SE01	iQ5 Optical System Software Security Edition, single workstation license
170-9780	iQ5 Multicolor Real-Time PCR Detection System, includes iCycler base, optics module, software CD-ROM (standard edition), 5 installed filter sets, 96-well reaction module, calibration solutions, optical-quality 96-well PCR plates, Microseal 'B' seals, communication cables, power cord, quick reference cards, instructions

The Gene Expression Gateway

One Click to Bio-Rad's Genomics Expertise

Your gateway to Bio-Rad's extensive genomics expertise is just a mouse-click away.

- Technical notes covering a broad range of genomics applications
- Abstracts for over 10,000 research articles that relied on Bio-Rad products
- Practical information on the latest techniques — fast PCR, 5-target qPCR multiplexing, siRNA delivery, and much more

Visit the Gene Expression Gateway on the Web at **www.bio-rad.com/genomics/**

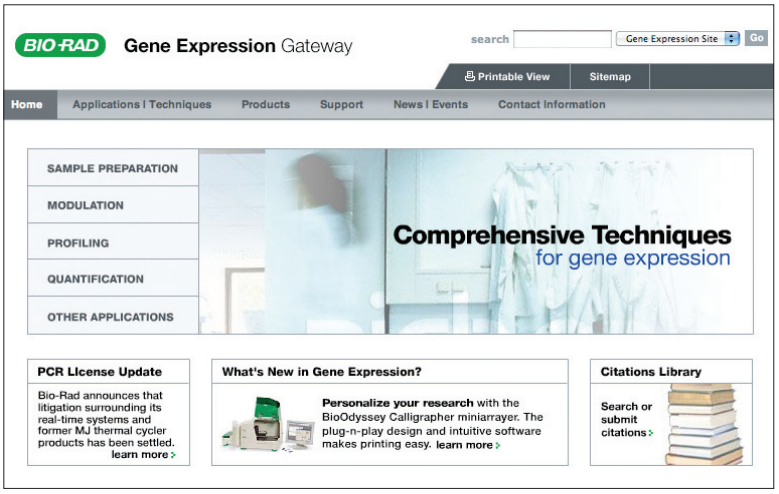

ProteOn™ XPR36 Protein Interaction Array System

The Power of Parallel Processing

Bio-Rad's portfolio of proteomics workflow solutions now includes the ProteOn XPR36 system, a surface plasmon resonance optical biosensor. Take the next step from protein discovery to function with the ProteOn XPR36, a label-free protein-protein interaction analysis system offering XPR™ technology, a unique 6 x 6 crisscross approach to multiplexing.

XPR technology offers the ability to monitor up to 36 different interactions in real time through the parallel processing of six different ligands with six different analytes.

Product Offering Includes

- ProteOn XPR36 optical biosensor
- ProteOn™ Manager software for instrument control, data collection, and analysis
- Controller and display
- Selection of sensor chip surfaces for a variety of applications
- Protocol development kits
- Reagents and kits for coupling, regeneration, maintenance, and verification

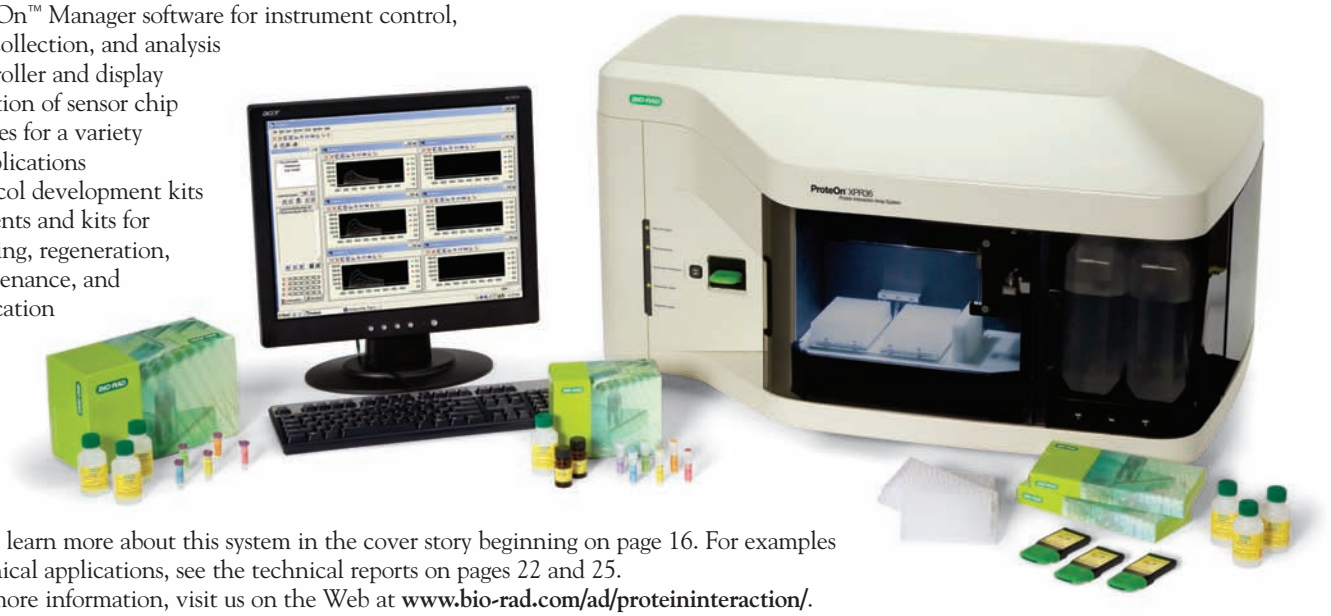

You can learn more about this system in the cover story beginning on page 16. For examples of technical applications, see the technical reports on pages 22 and 25.

For more information, visit us on the Web at **www.bio-rad.com/ad/proteininteraction/**. For product availability in your area, contact your local Bio-Rad sales representative.

Amplification

- Analysis of chromatin transitions by real-time quantitative PCR (bulletin 5371; PDF only)
- Gene expression profiling brochure (bulletin 5373)
- Fast PCR: general considerations for minimizing run times and maximizing throughput (bulletin 5362)

Chromatography

- Automated three-dimensional purification method for histidine-tagged proteins using the BioLogic DuoFlow Maximizer™ chromatography system (bulletin 5342)
- BioLogic DuoFlow™ system brochure (bulletin 5369)
- Bio-Scale™ Mini Profinity™ IMAC product information sheet (bulletin 5444)
- Connecting Bio-Rad columns to GE Healthcare systems, and GE Healthcare columns to Bio-Rad systems (bulletin 5326)
- Method for packing Macro-Prep® High S resin in pilot- and process-scale columns (bulletin 5384)
- Method for packing CHT™ ceramic hydroxyapatite Type I, 40 µm, in GelTec™ columns (bulletin 5357)
- Method for packing UNOsphere™ S cation exchange support in pilot- and process-scale columns (bulletin 5385)

Electrophoresis

- Experion™ automated electrophoresis system and the Experion Pro260 analysis kit: accurate and reproducible protein sizing and quantitation in the presence of high salt concentrations (bulletin 5328)
- Experion system product information sheet (bulletin 5340)
- Gene expression profiling brochure (bulletin 5373)
- Protein quantitation: a comparative analysis using the Experion automated electrophoresis system, Bradford and modified Lowry assays, and SDS-PAGE (bulletin 5423)
- RNA quantitation: a comparative analysis using the Experion automated electrophoresis system, RiboGreen reagent, and ultraviolet spectroscopy (bulletin 5420)

Gene Transfer

- RNAi brochure (bulletin 5270)

Imaging

- Using the Molecular Imager® PharosFX™ system to image arrays printed with the BioOdyssey™ Calligrapher™ miniarrayer (bulletin 5436)
- BioOdyssey Calligrapher miniarrayer applications: screening for gene silencing (bulletin 5437)

Microarray Products

- DNA microarrays: optimization of fabrication parameters and control plate design (bulletin 5308)
- Gene expression profiling brochure (bulletin 5373)

Multiplex Suspension Array Technology

- Bio-Plex™ system family brochure (bulletin 5405)
- Bio-Plex system nucleic acid application paper (bulletin 5336; PDF only)

Protein Interaction Analysis

- ProteOn system folder (bulletin 5434A)
- ProteOn XPR36 protein interaction array system brochure (bulletin 5390)
- Rapid and efficient determination of kinetic rate constants using the ProteOn XPR36 protein interaction array system (bulletin 3172)
- Mechanisms of protein-protein binding: double-mutant cycle analysis (bulletin 5358)
- Rapid and detailed analysis of multiple antigen-antibody pairs using the ProteOn XPR36 protein interaction array system (bulletin 5360)
- Rapid optimization of immobilization and binding conditions for kinetic analysis of protein-protein interactions using the ProteOn XPR36 protein interaction array system (bulletin 5367)
- Analysis of multiple protein interactions using the ProteOn XPR36 protein interaction array system (bulletin 5368)

Sample Preparation

- Enriching basic and acidic rodent brain proteins with ion exchange spin columns for two-dimensional gel electrophoresis (bulletin 5398)

Convenient Multiplex PCR Assays With iQ™ Multiplex Powermix

Liz Jordan and Naheed Aslam, Bio-Rad Laboratories, Inc., Hercules, CA 94547 USA

Multiplex Quantitative Studies of Gene Expression

Gene expression analysis is a fundamental element of research on disease and drug development. To study gene expression, the corresponding mRNA levels must be assessed either quantitatively or qualitatively. One reliable method of assessment is reverse transcription of the mRNA into copies of DNA (cDNA) using reverse transcriptase, followed by quantitation of the cDNA using quantitative PCR. Reverse transcription-quantitative PCR (RT-qPCR) has been used for validating expression results obtained from microarrays as well as for more detailed quantitation.

Absolute quantitation of gene expression results in limited information about the transcripts of a specific gene. More relevant information can be obtained from relative gene expression studies in which one looks at internal reference gene(s) within the sample to normalize the relative change in the gene of interest (Bustin 2000, Vandesompele et al. 2002). Determination of relative gene expression can be accomplished by setting up separate reactions to analyze the gene of interest and the internal reference gene (this is required when using SYBR Green I); alternatively, the target genes can be amplified concurrently in a single reaction tube (referred to as multiplexing). In addition to gene expression analysis, multiplex real-time PCR has been used to detect different bacteria in the same sample (Templeton et al. 2003, 2004, Khanna et al. 2005), to detect mutations in more than one PCR product (Uggozoli et al. 2002), and to analyze multiple transcripts in the same sample (Persson et al. 2005). The advantage of performing multiplex qPCR assays is that one can assess up to five different PCR products in the same tube (using the iQ™5 multicolor real-time PCR detection system). Thus, it is possible to assess several internal reference genes and genes of interest in the same tube, using much less sample than when each reaction is set up individually.

To multiplex, each PCR product requires a gene-specific primer set and a fluorophore-labeled gene-specific probe along with standard PCR reagents. Until recently, qPCR multiplexing was accomplished by supplementing a real-time 2x supermix with additional dNTPs, $MgCl_2$, and *Taq* polymerase, so that limiting reagents would not influence any of the reactions. Another approach sometimes used in optimizing multiplex reactions is to determine the limiting primer concentration for the more highly expressed targets by testing a series of concentrations. This approach conserves reagents so that amplification of lower-abundance targets can occur unhindered. This practice not only is time consuming, but also uses more of the required reagents. Bio-Rad recently introduced iQ multiplex powermix to provide exceptional multiplexing results for up to five unique targets with minimal need for optimizing reaction conditions, allowing considerable savings in cost and time.

This article describes several points that must be addressed for optimal multiplexing of reactions.

Guidelines for Experimental Design

Primers, Probes, and Internal Reference Genes

Primers and their associated probes should be designed at the same time, but only the primers should be ordered for the initial validation experiments (see next section). It is often advisable to design several primer and probe sets per PCR product, and order and validate the primer sets first.

It is critically important in qPCR multiplex assays that there be no complementarity between any of the primers and probes that will be included in the reaction. During the experimental design stage, it is important to assess all the primer and probe sequences for complementarity. A convenient rule of thumb is to have no more than four complementary bases in a row, to avoid any possible cross-hybridization. Many tools are available to test these interactions and assist in the design of multiplex reactions, including oligonucleotide design web sites and more extensive software packages such as Beacon Designer. This software will perform all pairwise comparisons and will suggest only primers and probes that will not cross-hybridize with each other.

Another important experimental design consideration is the choice of appropriate internal reference genes for normalizing sample input across treatment conditions or samples (Bustin

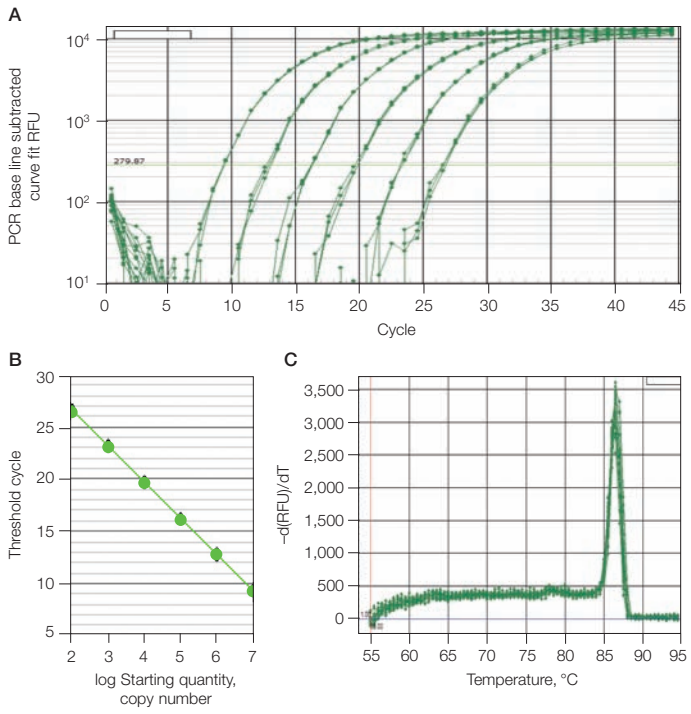

Fig. 1. SYBR Green I assay validation and melt curve for the β-actin primer set. **A**, amplification curve for 10-fold serial dilutions of β-actin plasmid (10^7–10^2 copies per reaction); **B**, resulting standard curve with efficiency = 94.6%, slope = –3.459, R^2 = 1.00; **C**, melt curve run immediately after amplification.

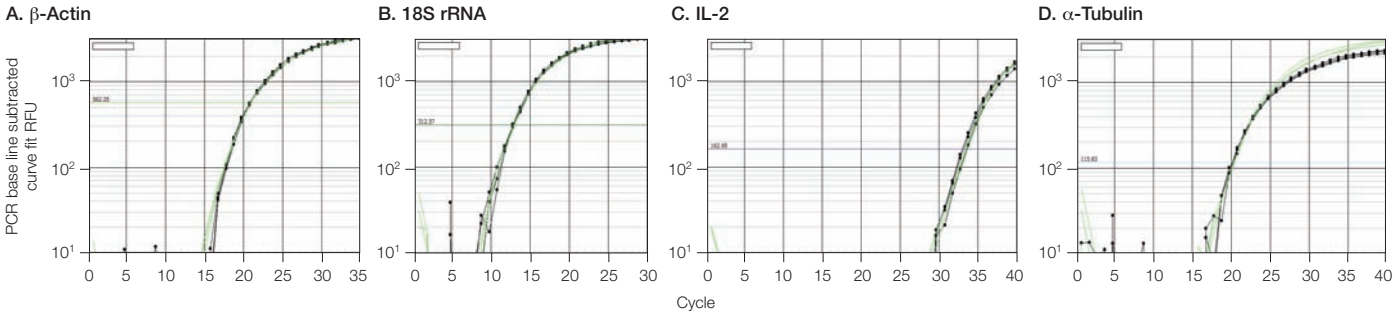

Fig. 2. Comparison of singleplex and multiplex results. Template was human spleen cDNA prepared from purchased RNA, using iScript™ reverse transcriptase. One-tenth of a 1 µg cDNA synthesis reaction was added to each 50 µl reaction. (■), multiplex reactions; (—), singleplex reactions. **A**, β-actin primers and FAM-labeled probe; **B**, 18S rRNA primers with HEX-labeled probe; **C**, interleukin-2 (IL-2) primers and Texas Red-labeled probe; **D**, α-tubulin primers with Cy5-labeled probe.

2000). Several researchers have investigated the use of appropriate housekeeping genes in detail, suggesting that up to three internal reference genes be used to reduce the likelihood of incorporating large errors into the results (Vandesompele et al. 2002). These internal reference genes must be shown to be stably expressed across the proposed experimental conditions (Livak and Schmittgen 2001, Guo et al. 2002).

Validation of Primer and Probe Specificity and Efficiency

Each real-time reaction should be characterized individually using SYBR Green I before ordering the probe. By doing so, if primers need to be redesigned, one will not incur the added potential cost of probe redesign. Figure 1 shows an example of a reaction run with SYBR Green I to determine reaction efficiency, with melt-curve analysis to show specificity. The melt curve shows the absence of primer-dimers even at low template concentrations. The reaction efficiency is calculated from the slope of the standard curve (expected efficiency >90%). In the case shown, the efficiency was 94.6%.

Specificity (amplification of only one PCR product) is verified using melt-curve analysis as well as by running representative samples on a high-resolution gel. The optimal annealing temperature of the primers can be determined using the gradient feature included in iCycler iQ®, MyiQ™, iQ5, and Opticon Monitor™ software. Primer and $MgCl_2$ concentrations can also be titrated to improve reaction efficiencies. If none of these methods results in adequate reaction optimization, we recommend redesigning the primers.

When both the reaction efficiency and the specificity are acceptable, probes should be ordered and validated over the relevant template concentration range. These assays should display the same performance with the probe as with SYBR Green I (>90% efficiency for each reaction). Because the goal of a multiplex gene expression experiment is to compare expression levels of a gene of interest to a reference gene, it is important that the efficiencies of all reactions be similar to one another (generally within 5%).

Multiplex Reactions

Once all individual reactions have been tested, it is important to compare the individual reactions with the multiplex reaction. This comparison will expose any effects of one reaction on the others in the multiplex reaction. There should be no significant difference between the threshold cycle (C_T) value obtained for a reaction in the singleplex format and the value obtained in the multiplex format. If this is not the case, further investigation of primer interactions will be necessary.

Figures 2 and 3 display a validation experiment showing that the C_T of each singleplex reaction does not shift when the same assay is performed in a four-target multiplex reaction. Each of the singleplex reactions was previously validated following the strategies described above. Amplification was performed using iQ multiplex powermix and the same primer (300 nM) and probe (200 nM) concentrations for singleplex and multiplex reactions. We recommend running a two-step PCR protocol (combining the annealing and extension steps) and allowing adequate time (about 1 min) for the instrument to collect data through all four or five filter sets.

These data demonstrate that each of the singleplex reactions performs similarly whether run independently or in the four-target multiplex assay. Additionally, the difference in C_T values of 20.6 between the 18S rRNA (HEX) and IL-2 (Texas Red) traces (Figure 3) represents over 6 orders of magnitude difference in template concentration, yet the presence of more highly expressed targets had no effect on the amplification of IL-2. From these data, we have determined that multiplexing these reactions will not skew our data on the relative expression of one gene compared with the others. Furthermore, no additional optimization was required when using iQ multiplex powermix.

Table 1 shows the average C_T values obtained for four replicate amplifications using each primer/probe set in singleplex and corresponding multiplex reactions. The C_T values are essentially the same when including the SD; there is a slight shift of ~0.12 C_T for α-tubulin, which is acceptable.

At this point, the validation of our model system has led to an optimized experimental design for gene expression studies. Modifications of the $2^{-\Delta\Delta C_T}$ method (Livak and Schmittgen 2001, Vandesompele et al. 2002) are most often used to present relative gene expression data. Figure 4 illustrates the type of relative and

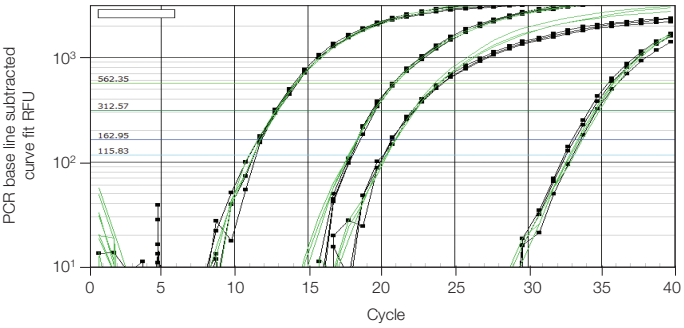

Fig. 3. Multiplex reactions showing all four fluorophore traces on the same graph. From left to right: 18S rRNA (HEX), β-actin (FAM), α-tubulin (Cy5), and IL-2 (Texas Red). Data set is the same as in Figure 2.

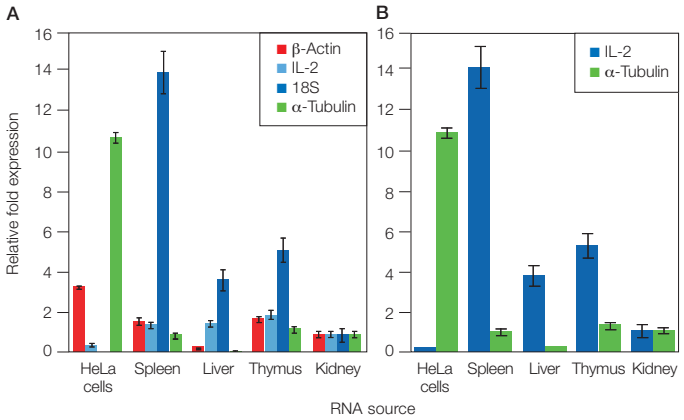

Fig. 4. Four-color multiplex reactions carried out using cDNAs prepared from different RNA sources. Reactions were carried out in triplicate with one-tenth of a 1 µg cDNA synthesis reaction using total human RNA in each 50 µl reaction. Genes analyzed were β-actin, 18S rRNA, IL-2, and α-tubulin. Kidney was set as the control sample. **A**, relative quantity (ΔC_T) relative to zero; β-actin and 18S were used as reference genes for this analysis. **B**, normalized expression data ($\Delta\Delta C_T$).

Table 1. Comparison of C_T of each reaction in singleplex and multiplex. Values shown are averages ± SD.

Target	Singleplex	Multiplex
β-Actin	20.89 ± 0.07	20.82 ± 0.08
18S rRNA	12.85 ± 0.07	12.82 ± 0.08
IL-2	33.46 ± 0.18	33.21 ± 0.30
α-Tubulin	20.27 ± 0.04	20.09 ± 0.02

normalized gene expression graphs that can be displayed with iQ5 software. The data suggest that HeLa cells express about 8 times more α-tubulin than kidney, and spleen expresses about 8 times more IL-2 than kidney.

iQ multiplex powermix permits multiplexing of five PCR products in a single tube (Figure 5). Singleplex assays run alongside the five-color multiplex assay verified that there was no significant difference in C_T values between the two formats. In contrast, when another commercially available supermix designed for multiplex qPCR was used, there was a shift in C_T values between singleplex and multiplex reactions for targets expressed at low levels (Figure 6B). Therefore, the reaction would require further optimization. Analysis of this suboptimal multiplex data might cause one to conclude that α-tubulin is expressed over 100-fold lower relative to singleplex data, and normalized to β-actin and 18S rRNA expression levels.

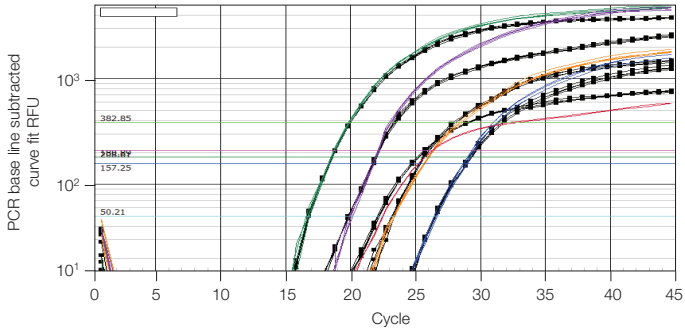

Fig. 5. Five-target multiplex reaction. One-tenth of a 1 µg cDNA synthesis reaction of human spleen total RNA was used in each 50 µl reaction. (■), multiplex; singleplex reactions: (—), FAM-labeled β-actin probe; (—), Cy5-labeled α-tubulin probe; (—), TET-labeled GAPDH probe; (—), TAMRA-labeled cyclophilin probe; (—), Texas Red-labeled IL-2 probe.

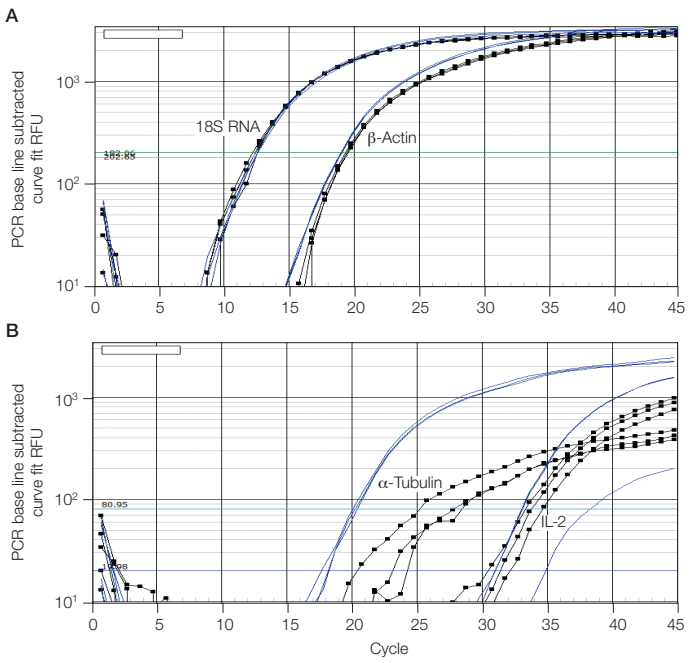

Fig. 6. Four-target multiplex reactions with another supplier's reagent are not as robust for low-expression targets. One-tenth of a 1 µg cDNA synthesis reaction was used in each 50 µl reaction. Genes analyzed were β-actin (FAM), 18S rRNA (HEX), α-tubulin (Cy5), and IL-2 (Texas Red), and the experiment was performed according to the supplier's protocol. (■), multiplex; (—), singleplex reactions. The four traces are plotted in two panels for clarity: higher-expressing targets are shown in **A**, lower-expressing targets in **B**.

Conclusions

Multiplexing requires some initial optimization of individual reactions. Once the assays have been validated, multiplexing is a powerful tool that can provide a large amount of data from small sample quantities. The extensive versatility of iQ multiplex powermix reduces the need to optimize multiplex reaction conditions.

References

Bustin SA, Absolute quantification of mRNA using real-time reverse transcription polymerase chain reaction assays, J Mol Endocrinol 25, 169–193 (2000)

Guo et al., The iCycler iQ detection system for evaluating reference gene expression in normal human tissue, Bio-Rad bulletin 2804 (2002)

Khanna M et al., The pneumoplex assays, a multiplex PCR-enzyme hybridization assay that allows simultaneous detection of five organisms, *Mycoplasma pneumoniae*, *Chlamydia* (*Chlamydophila*) *pneumoniae*, *Legionella pneumophila*, *Legionella micdadei*, and *Bordetella pertussis*, and its real-time counterpart, J Clin Microbiol 43, 565–571 (2005)

Livak KJ and Schmittgen TD, Analysis of relative gene expression data using real-time quantitative PCR and the $2^{-\Delta\Delta C_T}$ method, Methods 25, 402–408 (2001)

Persson K et al., Four-color multiplex reverse transcription polymerase chain reaction — overcoming its limitations, Anal Biochem 344, 33–42 (2005)

Templeton KE et al., Rapid and sensitive method using multiplex real-time PCR for diagnosis of infections by influenza A and influenza B viruses, respiratory syncytial virus, and parainfluenza viruses 1, 2, 3, and 4, J Clin Microbiol 42, 1564–1569 (2004)

Templeton KE et al., Development and clinical evaluation of an internally controlled, single-tube multiplex real-time PCR assay for detection of *Legionella pneumophila* and other *Legionella* species, J Clin Microbiol 41, 4016–4021 (2003)

Uggozoli LA et al., Fluorescent multicolor multiplex homogeneous assay for the simultaneous analysis of the two most common hemochromatosis mutations, Anal Biochem 307, 47–53 (2002)

Vandesompele J et al., Accurate normalization of real-time quantitative RT-PCR data by geometric averaging of multiple internal control genes, Genome Biol 3, research0034.1–0034.11 (2002)

Monitoring the Expression, Purification, and Processing of GST-Tagged Proteins Using the Experion™ Automated Electrophoresis System

Xuemei He and William Strong, Bio-Rad Laboratories. Inc, Hercules, CA 94547 USA

Introduction

Expression and purification of recombinant proteins are prerequisites for their structural and functional characterization, and affinity tag systems have become the predominant approach for obtaining highly purified target proteins. Among the widely used affinity tags, the glutathione S-transferase (GST) sequence has been shown to stabilize and, in some cases, improve the solubility of recombinant proteins (Terpe 2003); however, this 26 kD tag is immunogenic and may interfere with the structure or biological activity of target proteins, thereby necessitating its removal. Thrombin is a protease commonly employed for this purpose and, if biotinylated, it can be removed from a digestion mixture using *Strep*-tag/StrepTactin chromatography or streptavidin agarose (Terpe 2003). Nevertheless, complications may arise during the purification of GST fusion proteins and subsequent affinity tag removal, such as copurification of host proteins that interact with the GST domain (Lichty et al. 2005) or poor efficiency and specificity of protease activity (Chang et al. 1985, Jenny et al. 2003). The purification of GST fusion proteins, therefore, must somehow be monitored at each step.

We have used the Experion automated electrophoresis system and Experion Pro260 analysis kit to monitor the expression of GST-tagged proteins in *E. coli* and to analyze samples from the purification and processing of these proteins (He and Strong 2005). Here, we present a portion of our results to demonstrate that the Experion system offers data with quality comparable to that generated by traditional sodium dodecyl sulfate-polyacrylamide gel electrophoresis (SDS-PAGE) while eliminating the laborious procedures associated with gel electrophoresis.

Methods

Expression of Fusion Protein PPPS50-GST

A GST fusion of a proprietary recombinant protein, PPPS50 (50 kD), was used in these studies. *E. coli* BL21(DE3) cells harboring the PPPS50-GST expression plasmid were grown at 28°C in Terrific Broth containing 100 µg/ml ampicillin. Expression was induced by 0.1 mM isopropyl-β-D-1-thiogalacto-pyranoside (IPTG). Cells were harvested 3 hr after induction.

Purification of PPPS50-GST

The frozen *E. coli* BL21(DE3)-PPPS50-GST cell paste (0.4 g) was resuspended in 4 ml 1x GST bind/wash buffer (from the GST•Bind buffer kit, EMD Biosciences, Inc.) containing 2 µl/ml Lysonase bioprocessing reagent (EMD Biosciences, Inc.). Following incubation at room temperature for 20 min, insoluble cell debris was removed by centrifugation, and PPPS50-GST fusion protein was purified from 200 µl crude extract using a GST MicroSpin column (GE Healthcare) following the manufacturer's instructions. Samples were taken during this purification process, frozen, and stored at –20°C.

Thrombin Digestion of PPPS50-GST

To determine the efficiency of fusion protein cleavage by biotinylated thrombin, digestion reactions containing increasing amounts of the enzyme were prepared. The 1 U/µl biotinylated thrombin stock (thrombin cleavage capture kit, EMD Biosciences, Inc.) was diluted to give a series of solutions containing 0.01–0.2 U/µl enzyme, and for each concentration, a 10 µl digestion reaction was prepared to contain 1 µl biotinylated thrombin solution, 1 µl 10x thrombin cleavage buffer, and 64 µg purified PPPS50-GST fusion protein. The reactions were incubated at room temperature for 2 hr. In a separate reaction, 5 U biotinylated thrombin was mixed with 8 mg purified PPPS50-GST and 10x thrombin cleavage buffer into a final volume of 250 µl. Aliquots of this reaction (50 µl) were removed after 0.5, 1, 2, 3, and 20 hr of incubation at room temperature. The extent of fusion protein cleavage in each reaction was determined using the Experion Pro260 analysis kit and by SDS-PAGE.

Stepwise Purification of PPPS50

Tag-free PPPS50 was purified in a stepwise fashion that involved cleavage of purified PPPS50-GST with biotinylated thrombin followed by thrombin removal with streptavidin agarose, desalting with Bio-Gel® P-6 support, and removal of the GST tag by affinity chromatography using GST MicroSpin columns. First, purified PPPS50-GST (8 mg) was mixed with 25 µl 10x thrombin cleavage buffer and 5 U biotinylated thrombin in a final volume of 250 µl and incubated at room temperature for 18 hr. A 30 µl sample was taken at the time of completion. To the rest of the reaction, 160 µl streptavidin agarose (50% slurry, from the thrombin cleavage capture kit) was added, and this mixture was incubated at room temperature for 30 min. The streptavidin agarose was then removed with a spin filter according to the manufacturer's instructions. A 27 µl sample was taken from the filtrate for analysis with the Experion system and by SDS-PAGE.

The thrombin-free sample was desalted on Micro Bio-Spin™ 6 columns, which are packed with Bio-Gel P-6 support, and then applied onto a freshly equilibrated GST MicroSpin column. The released GST tag was captured by the column, and the tag-free PPPS50 was collected in the flow-through fraction. Samples of both the bound and flow-through fractions were analyzed with the Experion system and by SDS-PAGE.

Experion Pro260 Analysis

Samples were prepared according to the instructions provided in the Experion Pro260 analysis kit instruction manual for protein separation under reducing conditions. Samples (4 µl) were used without dilution. Protein purity and relative quantitation values were automatically calculated by Experion software.

SDS-PAGE Analysis

Samples were prepared by mixing 4 µl of each protein solution with an equal volume of 2x Laemmli sample buffer containing 5% β-mercaptoethanol, and were heated at 95°C for 5 min prior to being loaded onto gels. SDS-PAGE was performed in a Criterion™ electrophoresis cell with 4–20% Criterion Tris-HCl precast gels under denaturing conditions. Gels were stained for 1 hr at room temperature with Bio-Safe™ Coomassie G-250 stain and destained in water overnight. Gels were imaged with a GS-800™ densitometer and analyzed with Quantity One® 1-D analysis software.

Results and Discussion

Monitoring Digestion of PPPS50-GST With Biotinylated Thrombin

Expression of the 76 kD fusion protein, PPPS50-GST, was monitored using the Experion system and SDS-PAGE and was found to plateau 3 hr after IPTG induction, when it accounted for ~50% of the total protein (He and Strong 2005). Digestion of PPPS50-GST by biotinylated thrombin released the GST tag and the target protein, PPPS50. PPPS50-GST was cleaved quantitatively by undiluted biotinylated thrombin within 2 hr, while digestions using lower concentrations of biotinylated thrombin for the same period of time resulted in mixtures of full-length fusion protein and cleavage products (Figure 1). The enzyme could be effectively removed following a 20 hr incubation in which PPPS50-GST was fully processed by thrombin at one-fifth of its original concentration, and where no secondary digestion products were observed (Figure 2). The latter condition was adopted to minimize loss of target protein and to facilitate sample handling during removal of biotinylated thrombin with streptavidin agarose. Both the Experion system and SDS-PAGE offered high-quality data suitable for the kinetic study of this digestion (Figure 3). However, the Experion Pro260 analysis (which required only ~30 min for 10 samples) facilitated faster access to results and real-time monitoring of protein expression.

Monitoring Purification of Tag-Free PPPS50

A protocol for the large-scale purification of PPPS50 was generated using information gained from the above preliminary tests. Figure 4 shows separations of samples taken at various stages during this stepwise protein purification process. Note that, when using the Experion system to analyze protein samples, buffer exchange or desalting of samples prior to analysis may be necessary for optimal detection sensitivity or if absolute quantitation is desired. With the Experion system, charged proteins are electrokinetically injected into the separation channel of the microfluidic chip; therefore, the loading of proteins may be influenced by cellular or buffer components in the sample. Here, desalting enhanced the signal intensities of the

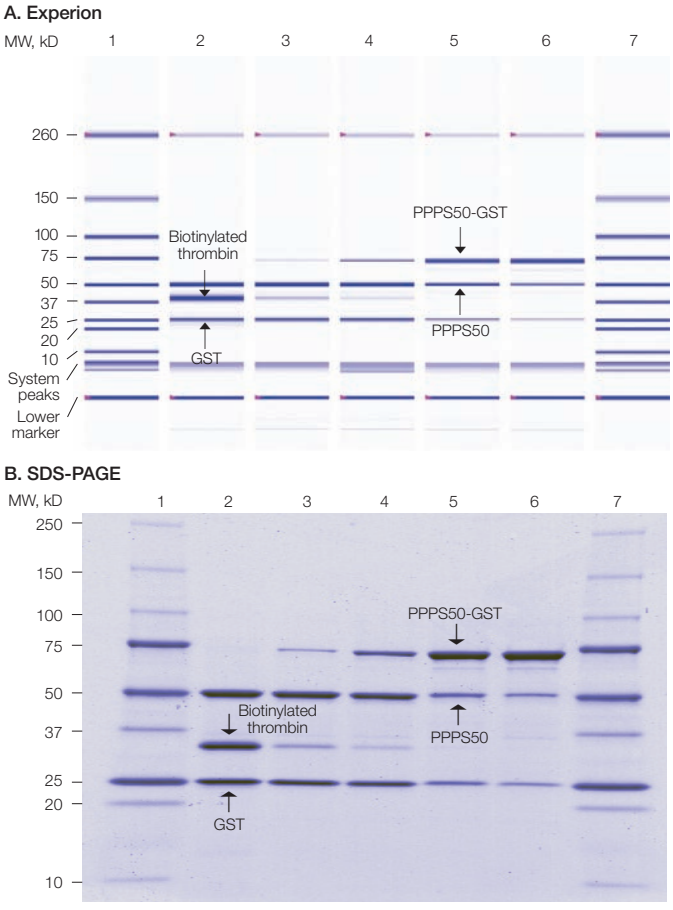

Fig. 1. PPPS50-GST cleavage by biotinylated thrombin. A, simulated gel image generated by the Experion system, showing separation of the Pro260 protein ladder in lanes 1 and 7; **B**, SDS-PAGE analysis, showing separation of the Precision Plus Protein™ standard in lanes 1 and 7. In both images, lanes 2–6 show the products from cleavage of 64 µg PPPS50-GST by 1, 0.2, 0.1, 0.02, or 0.01 U biotinylated thrombin after incubation at room temperature for 2 hr.

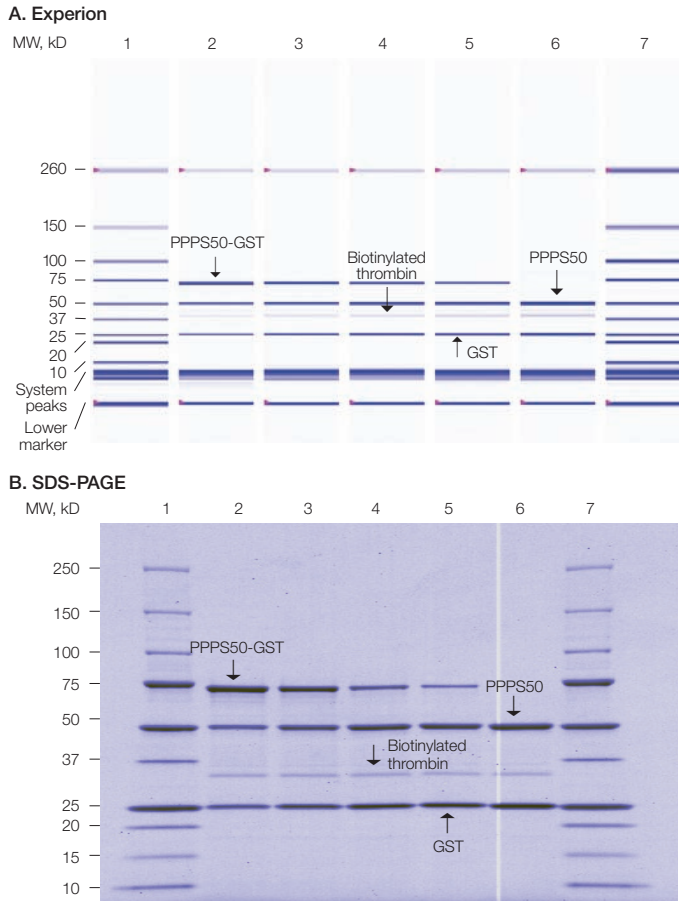

Fig. 2. Time dependence of PPPS50-GST cleavage by biotinylated thrombin. A, simulated gel image generated by the Experion system, showing separation of the Pro260 protein ladder in lanes 1 and 7; **B**, SDS-PAGE analysis, showing separation of the Precision Plus Protein standard in lanes 1 and 7. In both images, lanes 2–6 contain samples taken at 0.5, 1, 2, 3, or 20 hr of incubation at room temperature.

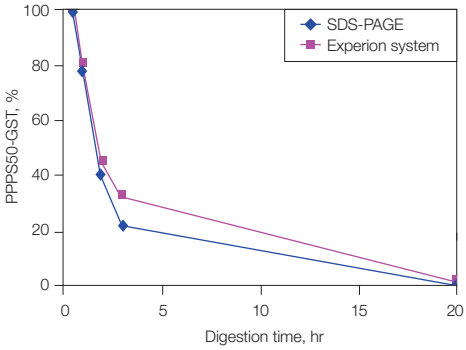

Fig. 3. Kinetics of PPPS50-GST cleavage by biotinylated thrombin at room temperature. Samples were analyzed with the Experion system or by SDS-PAGE. The relative amount of PPPS50-GST was expressed as a percentage of the amount at 0.5 hr.

samples analyzed with the Experion system (Figure 4A, lanes 8 and 9), but had little effect on the staining intensities of the samples separated by SDS-PAGE (Figure 4B, lanes 8 and 9).

The expression level of PPPS50-GST in *E. coli* BL21(DE3) cells, the purity of this fusion protein following purification on a GST MicroSpin column, and the purity of tag-free PPPS50 were determined with the Experion system and by densitometric scanning of SDS-PAGE gels (Table 1). The purity values obtained by the Experion system were generally in good agreement with those obtained by SDS-PAGE and Quantity One software analysis. The largest discrepancy was observed for the purity of PPPS50-GST in crude *E. coli* extracts (Table 1) and was likely due to inherent differences in the resolution offered by the two analytical methods. Whereas the Experion system demonstrated better resolution for 50 kD and larger proteins, SDS-PAGE provided excellent separation of smaller proteins. Accordingly, PPPS50-GST may have overlapped with other protein species of similar molecular weight on a 4–20% Tris-HCl gel, thereby contributing to its apparently higher abundance.

Using a 260 kD marker that is included in the Pro260 sample buffer at a known concentration, the Experion system provides automatic relative quantitation of protein samples, a feature that is not available with traditional SDS-PAGE. On the basis of the data reported by Experion software, the yield of PPPS50 from the postpurification processing of PPPS50-GST was ~87%; from 1 g fusion protein, ~870 mg PPPS50 could be obtained at a final concentration of 606 ng/µl.

Table 1. Stepwise purification and processing of PPPS50-GST.

	Experion System		SDS-PAGE	
Sample	Purity	Fold Purification	Purity	Fold Purification
Crude extract	14.0%	1.0	18.4%	1.0
PPPS50-GST	84.9%	6.1	86.6%	4.7
PPPS50	95.7%	6.8	97.3%	5.3

Conclusions

Qualitative and quantitative information about protein samples is valuable to the development of protein purification methods as well as to many downstream applications. The Experion system integrates protein separation, detection, and analysis within a single platform to reduce the amount of sample, reagents, and hands-on time required to perform routine qualitative and quantitative protein analyses. Experion analyses may be performed wherever the quality and/or quantity of protein samples must be assessed; in a purification scheme such as that described here, this means that the Experion system can save time analyzing samples during protein expression, optimization of purification methods, purification, and processing. This microfluidics-based system offers great convenience in sample analysis and a throughput unmatched by traditional SDS-PAGE.

References

Chang JY et al., Thrombin specificity. Selective cleavage of antibody light chains at the joints of variable with joining regions and joining with constant regions, Eur J Biochem 151, 225–230 (1985)

He X and Strong W, Monitoring the expression, purification, and processing of GST-tagged proteins using the Experion automated electrophoresis system, Bio-Rad bulletin 3176 (2005)

Jenny RJ et al., A critical review of the methods for cleavage of fusion proteins with thrombin and factor Xa, Protein Expr Purif 31, 1–11 (2003)

Lichty JJ et al., Comparison of affinity tags for protein purification, Protein Expr Purif 41, 98–105 (2005)

Terpe K, Overview of tag protein fusions: from molecular and biochemical fundamentals to commercial systems, Appl Microbiol Biotechnol 60, 523–533 (2003)

For an expanded version of this article, request bulletin 3176.

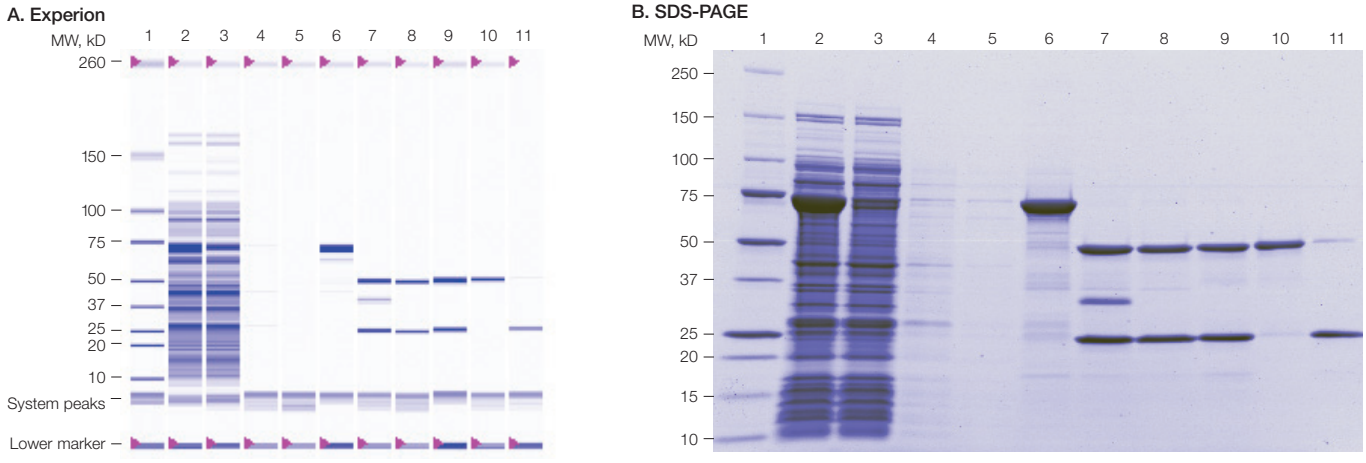

Fig. 4. Purification and processing of PPPS50-GST. A, simulated gel image generated by the Experion system, showing separation of the Pro260 protein ladder in lane 1; **B**, SDS-PAGE analysis, showing separation of the Precision Plus Protein standard in lane 1. In both images, lane 2 contains a separation of crude *E. coli* extract; lane 3, flowthrough from a GST MicroSpin column; lanes 4 and 5, fractions of unbound proteins washed from the column; lane 6, PPPS50-GST eluate; lane 7, products from biotinylated thrombin digestion of PPPS50-GST; lane 8, sample after biotinylated thrombin removal with streptavidin agarose; lane 9, sample after desalting with Micro Bio-Spin 6 columns; lane 10, tag-free PPPS50 collected in the flow-through fraction from a GST MicroSpin column; and lane 11, GST tag captured by the GST MicroSpin column.

Enriching Basic and Acidic Rodent Brain Proteins With Ion Exchange Spin Columns for Two-Dimensional Gel Electrophoresis

Ning Liu, Rose Gomez, Steve Freeby, Katrina Academia, Tim Wehr, Yuan Yan, Julie Hey, and Aran Paulus, Bio-Rad Laboratories, Inc., Hercules, CA 94547 USA

Introduction

Two-dimensional gel electrophoresis (2-DGE) can resolve up to a few thousand proteins in a single experiment with a dynamic range of detection typically within 2–4 orders of magnitude. The complexity of a protein sample can be reduced prior to 2-DGE to compensate for the limits of coverage and dynamic range. This can be accomplished by applying protein fractionation tools to the sample to allow analysis of one protein subset at a time, thereby increasing the load of proteins of interest and enriching low-abundance proteins. Ideally, such fractionation methods should be simple, fast, and efficient.

Here we discuss the chromatographic fractionation of proteins on Aurum™ ion exchange (IEX) mini spin columns containing either anion exchange (AEX) or cation exchange (CEX) media. By incorporating the IEX columns into a 2-DGE proteomics sample preparation workflow for analysis of rat and mouse brain proteins, more low-abundance proteins were detected in both the acidic and basic regions of the gels, allowing more effective probing for differential expression.

A proteomic method was developed using rat brain proteins and then applied to a biomarker study in a transgenic mouse model of Alzheimer's disease. The neurons of APP23 transgenic mice overexpress a mutant form of human amyloid precursor protein (APP), a key molecule implicated in this age-related, progressive neurological disorder (Sturchler-Pierrat et al. 1997). The APP23 transgenic mice exhibit Alzheimer's-like symptoms at 9 months but not at 3 months of age. We used brain tissues from 3-month-old control and APP23 transgenic mice for our study, with the aim of finding potential biomarkers associated with the early stages of the disease. Our results show that Aurum IEX mini spin columns are an effective way to fractionate complex protein mixtures and can improve detection of differentially expressed low-abundance proteins.

Methods

Fractionation of Rat Brain Proteins for 2-DGE

Figure 1 summarizes the general workflow and products used for the analysis of rat brain proteins. For enrichment of basic proteins, the pH of the protein samples was adjusted to 7.0 with 20 mM Bis-Tris for AEX columns or with 20 mM Na_2HPO_4 for CEX columns. For enrichment of acidic proteins, the pH of the protein samples was adjusted to 5.0 with 20 mM pyridine for AEX columns.

Following 2-DGE, spots excised from the gels were digested with trypsin, and digests were analyzed by reverse-phase liquid chromatography-mass spectrometry (LC-MS-MS) using an Agilent 1100 series capillary HPLC coupled to a Finnigan LTQ linear ion-trap mass spectrometer equipped with a nanoES ionization source (Thermo Electron Corp.). Proteins were identified by SEQUEST search of the rat.fasta database.

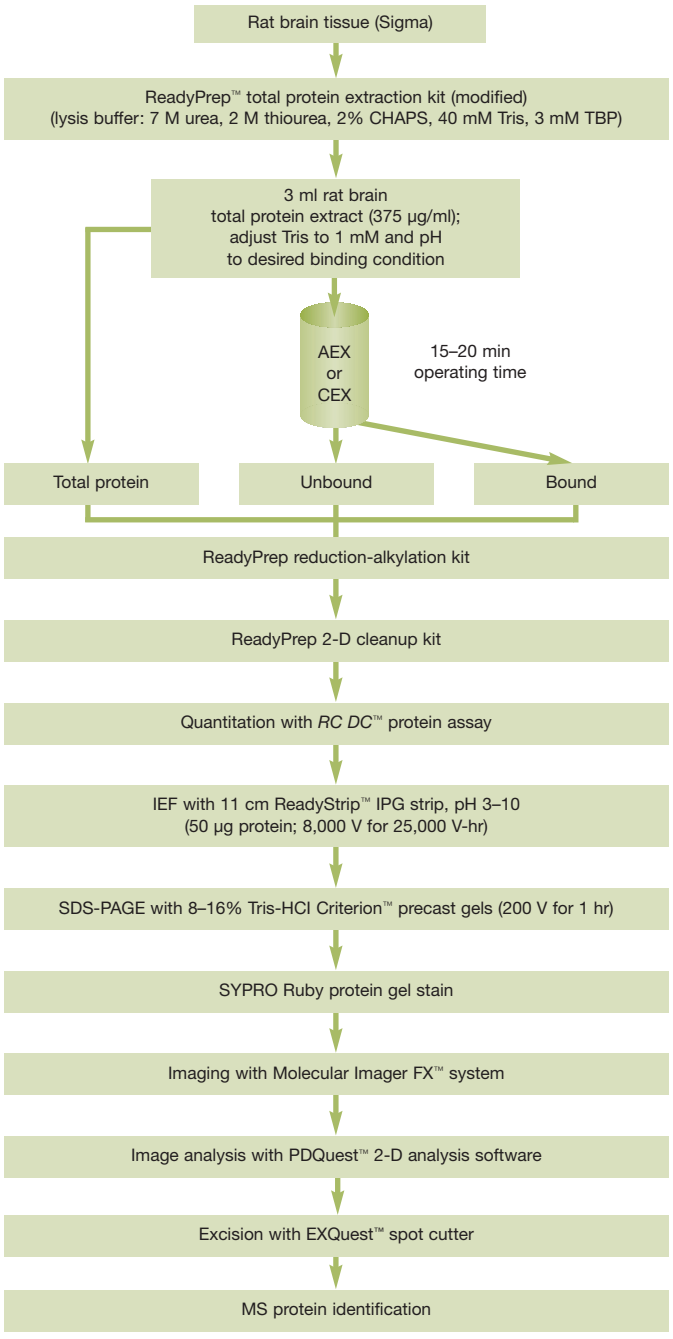

Fig. 1. 2-D analysis workflow using Aurum AEX or CEX columns for fractionation prior to 2-D gel analysis.

Comparison of Acidic Protein Profiles From Brains of Control and APP23 Transgenic Mice

Whole brain tissues from 3-month-old control and APP23 transgenic mice (kindly provided by Dr Rena Li, Sun Health Research Institute, Tucson, AZ) were homogenized in a buffer of 7 M urea, 2 M thiourea, 2% CHAPS, and 40 mM Tris. A 5 mg aliquot of each sample was treated with the ReadyPrep 2-D cleanup kit, separated on AEX columns at pH 5.0, and analyzed by 2-DGE and LC-MS-MS. Proteins were identified by SEQUEST search of the mouse.fasta database.

Results and Discussion

Enrichment of Basic Proteins at pH 7.0

Rat brain total protein extracts were fractionated by both IEX columns at pH 7.0 to enrich basic proteins. Both unbound and bound fractions were analyzed and compared to unfractionated samples by 2-DGE (Figure 2). PDQuest analysis of the gels revealed that 14% and 28% of the protein spots on the 2-D gels of the AEX unbound and CEX bound fractions, respectively, showed at least a 2-fold increase in intensity compared to the total protein gels, while 27% and 15%, respectively, were not observed at all on the total protein gels (see Table 1 for total spot counts).

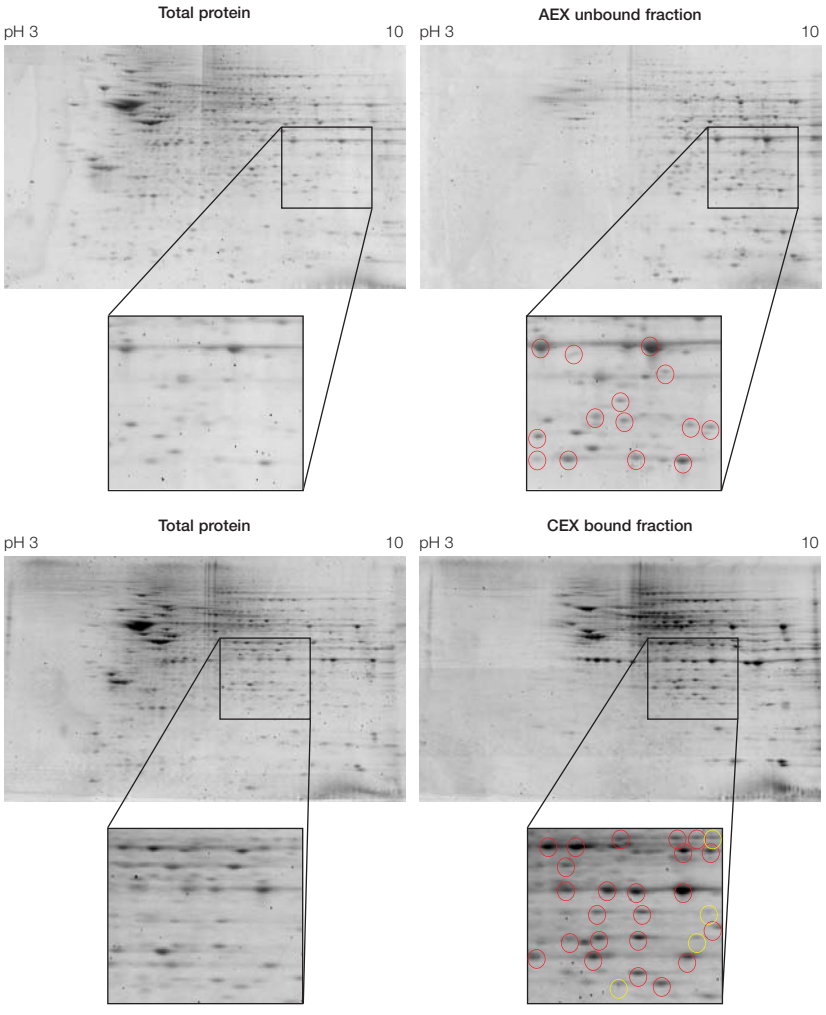

Fig. 2. Enrichment of basic proteins in rat brain after fractionation with Aurum AEX and CEX mini columns at pH 7.0. Red circles indicate protein spots with increased intensity compared to the total protein gels. Yellow circles indicate spots observed only in that gel. AEX bound and CEX unbound fractions not shown.

Table 1. Summary of numbers of protein spots detected.

	AEX Fractionation			CEX Fractionation		
	Total Protein	Unbound	Bound	Total Protein	Unbound	Bound
Total detected	557	247	550	428	418	391
At least 2x enrichment	—	34	66	—	61	109
At least 3x enrichment	—	11	22	—	19	46
Unique	—	66	112	—	69	59

Using MS, the identities of 14 of the protein spots from the CEX bound fraction gel were determined. The pIs of these proteins ranged from 6 to 10.7, demonstrating that the IEX mini spin columns can enrich basic proteins at pH 7.0 for 2-D gel analysis.

Enrichment of Acidic Proteins at pH 5.0

To enrich acidic proteins, rat brain total protein extracts were fractionated through AEX columns at pH 5.0. Again, both unbound and bound fractions were analyzed on 2-D gels and compared to the unfractionated sample (Figure 3). PDQuest analysis of the gels revealed 86 protein spots on the 2-D gel of the AEX bound fraction; in contrast, only 59 spots were found in the same pH range on the total protein gel. In the AEX bound fraction gel, 21 spots showed at least a 2-fold increase in intensity compared to the total protein gel, and 27 spots were observed only in the AEX bound fraction gel.

Reproducibility

To examine the reproducibility of this protein fractionation procedure, 5 mg of rat brain extract treated with the ReadyPrep 2-D cleanup kit was fractionated on three AEX columns at pH 5.0. The same amount of protein from each bound fraction was analyzed by 2-DGE in triplicate, and PDQuest software was used to match the protein spots among the gels. The correlation coefficients of these analyses between different groups of gels were very close to 1.0 (Table 2), indicating that the fractionation process was highly reproducible from column to column.

Application to Biomarker Discovery for Alzheimer's Disease

Control and APP23 transgenic mouse brain total protein lysates (5 mg each) were fractionated on AEX columns at pH 5.0, and the bound fractions from each sample were compared using larger PROTEAN® Plus 2-D gels (Figure 4). Again, the intensities of many of the protein spots on the 2-D gels of the AEX bound fractions were increased significantly compared to those on the total protein gels, and several low-abundance proteins were only detected on the gels of fractionated protein samples (Figure 4, red arrows).

One spot that had a significantly decreased intensity level in the APP23 transgenic mouse brain was identified by MS as tubulin β-2 (Figure 4, blue arrow). This form of tubulin β-2 focused at a position distinct from that of most tubulin β-2 proteins (Figure 4, black arrow), indicating

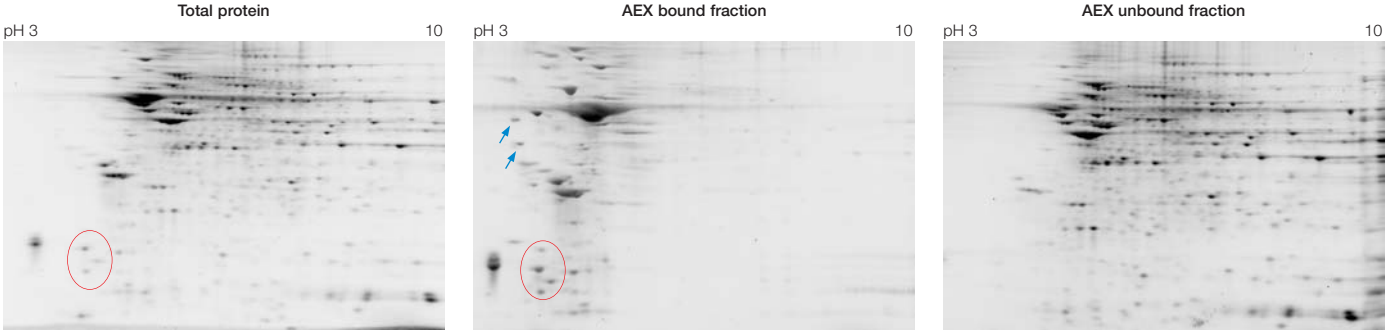

Fig. 3. Enrichment of acidic proteins in rat brain after fractionation with Aurum AEX mini spin columns at pH 5.0. Red circles indicate a group of protein spots with increased intensities after fractionation. Blue arrows show two representative spots detected only in the gels of the AEX bound fraction.

Table 2. Shown are the correlation coefficients from three AEX columns for a rat brain sample tested in triplicate by 2-DGE.

Spot Match Analysis	Correlation Coefficient
Columns 1 and 2	0.97
Columns 1 and 3	0.98
Columns 2 and 3	0.97

that it may have different posttranslational modifications than the other tubulins in brain cells. The level of this uniquely modified tubulin was decreased in the APP23 transgenic mouse brain, suggesting that microtubules, the major cytoskeleton component and transport system in cells, are altered by age 3 months in APP23 mice, even though the mice are symptom-free. This hypothesis is suggestive because microtubule malfunction in brain cells is associated with another well-known progressive neurological disorder, Huntington's disease. Future studies will need to be carried out to confirm this change in APP23 mice and to examine its involvement in the Alzheimer's disease mechanism.

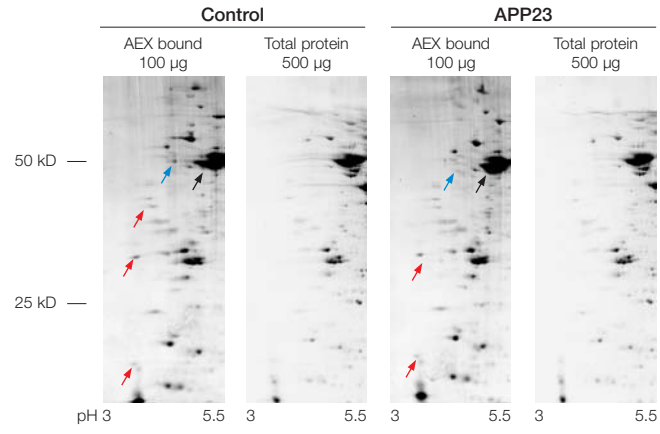

Fig. 4. Comparison of control and APP23 transgenic mouse brains with and without fractionation on AEX columns at pH 5.0. Red arrows, proteins detected only on gels of AEX fractionated sample; blue arrows, downregulated tubulin β-2 protein; black arrows, other tubulin β-2 proteins.

The differentially expressed tubulin β-2 protein was not apparent on the total protein gels of samples from either control or APP23 transgenic mice even though 500 µg was loaded, versus 100 µg on the gels of fractionated sample.

Conclusions

- Requiring only 15–20 min operating time, Aurum IEX mini spin columns provide a quick, convenient, and reproducible sample preparation tool for 2-DGE
- Fractionating rat and mouse brain total proteins with these columns improves detection of low-abundance proteins on 2-D gels and may facilitate the discovery of potential disease biomarkers in 2-D gel-based proteomics studies
- The identification of tubulin β-2 as a potential biomarker for Alzheimer's disease is promising. Future studies will need to be carried out to confirm the alteration of tubulin β-2 in APP23 transgenic mice and to examine its involvement in the Alzheimer's disease mechanism

Reference

Sturchler-Pierrat C et al., Two amyloid precursor protein transgenic mouse models with Alzheimer disease-like pathology, Proc Natl Acad Sci USA 94, 13287–13292 (1997)

For an expanded version of this article, request bulletin 5398.

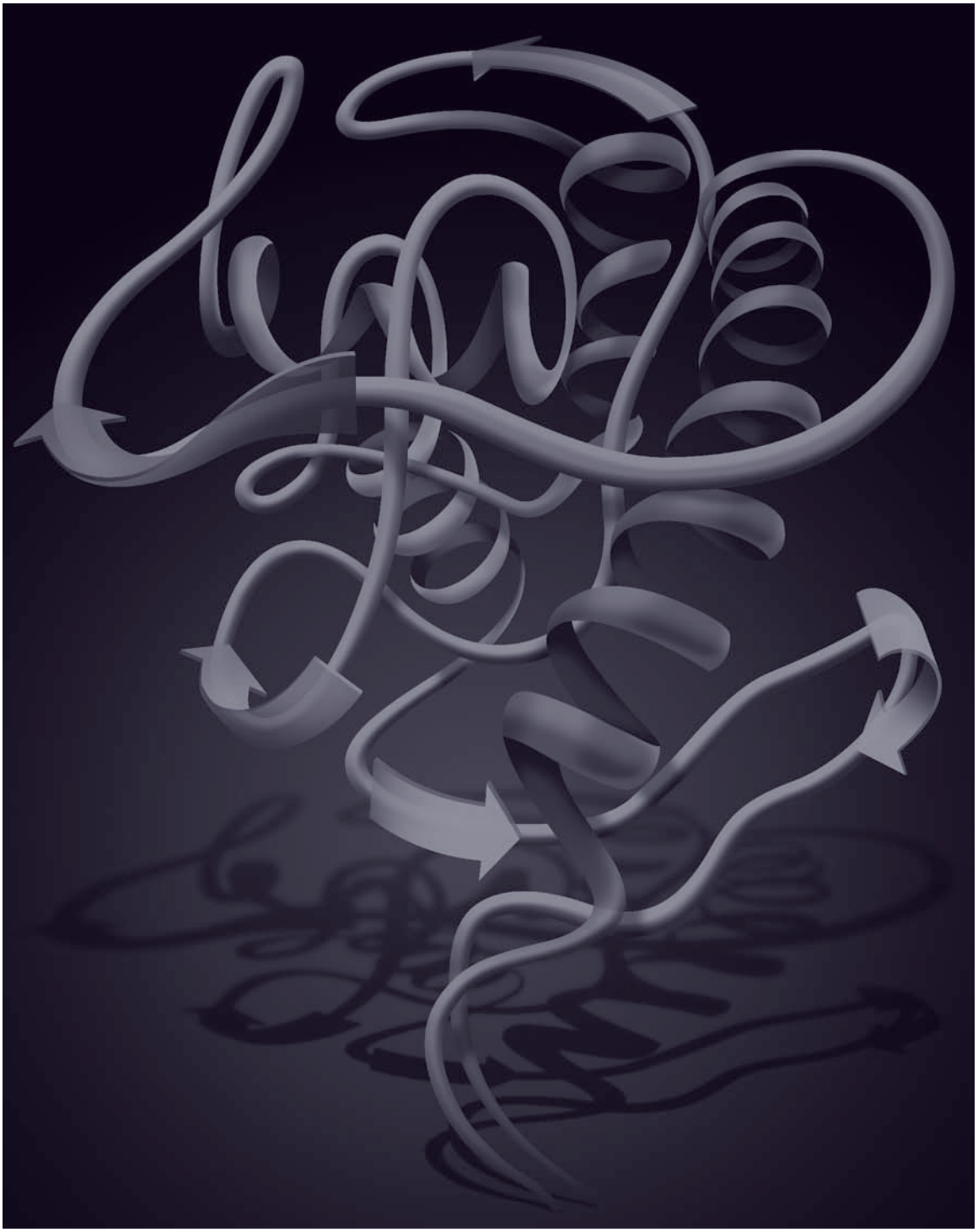

Author: Marty Bartholdi,
Bio-Rad Laboratories, Inc.,
Hercules, CA 94547 USA

Analyzing protein interactions with the ProteOn™ XPR36 protein interaction array system

Virtually every cellular structure and process depends on protein interactions. DNA replication and transcription, RNA splicing and translation, protein modification and secretion, cell cycle control and apoptosis, cell growth and intermediary metabolism, signal transduction, and gene expression — all exploit intricate protein interactions for the execution and maintenance of complex cellular life processes, making the analysis of protein interactions an especially valuable area of research.

Surface plasmon resonance (SPR) optical biosensing is an analytical technique that requires neither radiochemical nor fluorescent labels to provide real-time data on the affinity, specificity, and interaction kinetics of protein interactions. SPR biosensors generate the interaction data required to establish the functional roles of proteins, understand cellular function, and develop new drugs to treat disease (Rich and Myszka 2005).

This article introduces the ProteOn XPR36 interaction array system, an SPR imaging optical biosensor that allows simultaneous analysis of up to 36 biomolecular interactions on a single sensor chip. The ProteOn XPR36 system increases the throughput, flexibility, and versatility of experimental design for a wide range of biomolecular studies.

Evaluating Protein Interactions

Protein interactions are identified using a wide assortment of library-, affinity-, and array-based methods, such as yeast two-hybrid screening, protein arrays, proteolytic cleavage, and cross-linking. Identifying potential interacting partners, however, is only the first step towards understanding the impact of a protein interaction in the cell; also required is an understanding of the extent to which the interaction actually occurs. For this, the binding kinetics of the interaction as well as the environment of the interactants within a cell must be evaluated.

The Importance of Interaction Kinetics

To evaluate the strength of an interaction and the extent to which that interaction might occur in the cell requires an understanding of its kinetics. The strength of a two-molecule interaction is characterized by the equilibrium dissociation (binding) constant K_D = [P][L]/[PL], where [P] is the concentration of free protein, [L] the concentration of ligand, and [PL] the concentration of the complex. At equilibrium, K_D is related to the rate of complex formation (described by the association rate constant, k_a) and the rate of breakdown (described by the dissociation rate constant, k_d), such that $K_D = k_d/k_a$. A high-affinity interaction is characterized by a low K_D, rapid recognition and binding of the interactants (rapid "on rate", or high k_a), and stability of complex formation (slow "off rate", or low k_d) (Figure 1). Many commonly used techniques (for example, equilibrium dialysis and immunoprecipitation) provide measurements of K_D. However, most do not offer the real-time measurements required for determining association and dissociation kinetics.

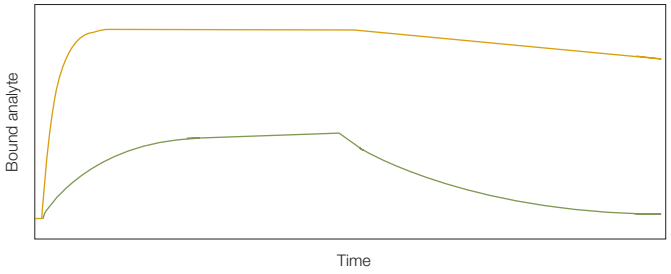

Fig. 1. Kinetics of analyte binding. Upper trace, a high-affinity interaction characterized by a high k_a (fast association) and a low k_d (slow dissociation); lower trace, a low-affinity interaction characterized by both a low k_a and a high k_d.

The measurement of relative association and dissociation kinetic rate constants is extremely valuable when investigating mutations of amino acid residues to study a protein interface or when modifying small-molecule lead compounds to optimize binding to drug targets. Changes made to interacting molecules may not affect overall binding affinity yet may alter the association and dissociation rates significantly. Since $K_D = k_d/k_a$, if both rate constants become slower or faster in concert after a molecular modification, then the contributions of particular residues or modifications may be overlooked if the binding constant alone is measured. When both the association and dissociation rates of an interaction are measured, insights can also be gained into the biological function of an interaction, the relevance of specific residues in binding hot spots can be determined, and compounds can be selected that bind to targets with clinically favorable properties.

Affinity data also provide an important clue as to whether two molecules actually interact in the intracellular milieu. For a protein and ligand to interact in a cell a significant fraction of the time, their intracellular concentrations must be in the same range as the K_D. The lower the value of K_D, the lower the concentration required for two intracellular proteins to interact; the higher the value of K_D, the higher must be their concentrations. Thus, affinity data combined with knowledge of intracellular concentrations provide an excellent diagnostic clue as to the biological relevance of intracellular protein interactions.

From protein interfaces to multiunit complexes and cascades, the ProteOn XPR36 system provides the high-quality data needed to decipher the fundamental interactions underlying protein function.

Considerations Related to Higher Levels of Cellular Organization

Even if a protein and its ligand exhibit strong binding affinity for each other and are expressed at sufficient levels in a particular tissue to interact functionally, other factors influence the nature of their interaction. Certain molecules, such as ions or cofactors, may be critical for binding, while others, such as competitors, can inhibit it. Molecular modifications, conformational changes, cellular compartmentalization, membrane dynamics, molecular crowding, or changes in pH of the cellular environment can also either promote or inhibit the interaction. There is, therefore, a well-established need to study protein interactions under biologically relevant, controlled conditions.

In addition, proteins are often part of functional networks made up of closely interacting clusters of proteins that in turn interact more loosely with other clusters (Spirin and Mirny 2003). The clusters correspond to protein complexes (proteins that form a functional unit) and dynamic cascades (proteins that execute a cellular process). SPR biosensors can provide useful data at this higher level of cellular organization by providing firm experimental data on the formation and stabilization of protein clusters. From such data, an understanding of the higher-level dynamics of functional networks becomes attainable.

SPR Optical Biosensors — Real-Time, Label-Free Kinetic Data

SPR optical biosensors respond with high sensitivity and in real time to the recognition, binding, and separation of two interacting molecules, which provides critical data regarding the rates of association and dissociation.

The principle behind SPR is detailed in the sidebar opposite. SPR biosensors analyze interactions free of radiochemical and fluorescent labels, bypassing the need for costly, time-consuming labeling reactions and eliminating the potential for unintentional modification of interacting chemical groups. SPR biosensors can detect subfemtomolar levels of proteins and other molecules as small as a few hundred Daltons, and are compatible with a wide range of biologically relevant chemical environments and temperatures. SPR biosensing is fast, requires very little material,

How SPR Can Reveal Protein Interactions

Surface plasmon resonance (SPR) is a phenomenon that occurs when light interacts with a metal film (such as gold) placed at the interface between two media with different refractive indices (such as a glass prism and water).

When light passing through glass crosses into water, it speeds up because the water has a lower refractive index. If the light is traveling at an angle when it crosses the interface, it will bend toward the glass (refract). At a single well-defined angle (the critical angle), the light cannot pass into the water and instead propagates along the interface. This light wave is called the evanescent wave. Because light has wavelike properties, however, a portion of the wave evanesces, or extends a fraction of a wavelength into the water before disappearing.

If a thin layer of gold is inserted between the glass and water, light incident at any angle onto the gold surface is reflected back into the glass. But the evanescent wave produced by the incident light is partly absorbed by the gold. Gold, like all metals, has the property that its electrons are not confined to a single nucleus but act as a charged "sea" that can respond in unison. Disturbance of the negatively charged electrons by the absorption of light causes a local charge imbalance, which causes waves of electrons to move with the waves of light. This effect is called surface plasmon resonance. Careful observation reveals a thin shadow in the reflected image at a specific angle corresponding to the absorption of the incident light by the gold surface. This shadow is called the SPR dip, and the angle at which the dip occurs (the SPR angle) can be measured by an optical detector.

SPR optical biosensors respond in real time to changes in the refractive index near the surface (in the range of the evanescent wave) resulting from the binding and subsequent separation of two proteins. One protein is chemically bound to the gold layer on the sensor surface, and a second protein flows in solution over the immobilized protein. As the protein in solution binds to the immobilized protein, the refractive index near the sensor surface increases, leading to a shift in the SPR angle. When the protein solution is replaced with a solution without protein, the protein complex on the sensor surface dissociates, the refractive index decreases, and the SPR angle shifts back.

SPR optical biosensors record the shift in the SPR angle as a function of time in the form of a sensorgram (see figure below). The angular shift is measured in response units (RU). (1 RU = 10^{-6} change in refractive index.) The sensorgram displays the time course of binding of analyte to ligand on the chip surface. During the association phase, analyte solution flows over the ligand surface and analyte binds to the ligand. If the association phase is sufficiently long, the reaction will reach a plateau (equilibrium) characterized by equal rates of association and dissociation. When analyte flow is stopped, the dissociation phase starts and the sensorgram declines as analyte leaves the ligand surface.

The shift in SPR angle can be measured so precisely that the binding kinetics of protein-protein interactions can be measured without labels at a resolution of detection on the order of picograms of protein per square millimeter of sensor surface.

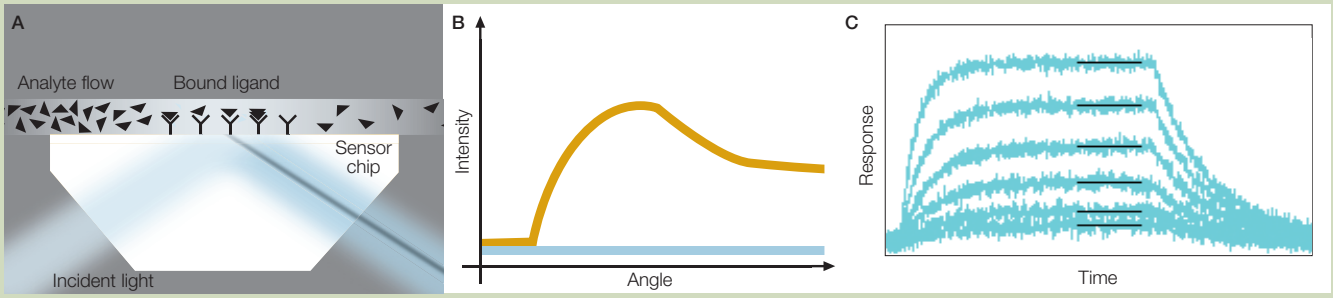

Schematic illustration of the conversion of shift in SPR angle to sensorgrams. A, as analyte binds to ligand molecules on the sensor chip surface, the intensity minimum (shadow) produced by the SPR effect shifts. **B**, this intensity shift is measured in real time for 36 interaction spots and 42 interspot references (shown for one spot). **C**, each of the resulting sensorgrams is fitted to an appropriate mathematical model to quantitatively characterize the interaction (shown for one set of 6).

and can be applied to studies of most biomolecules, including DNA, RNA, lipids, and carbohydrates as well as proteins. Using SPR biosensors, then, the native state of a protein can be simulated and modified as necessary to decipher the mechanisms of its interaction with other biomolecules.

SPR biosensors complement a number of techniques to effectively link interaction mechanisms with biological function. SPR biosensors are used for effective antibody characterization and development, and for the study of drug-target interactions. Used alongside other screening techniques, like yeast two-hybrid or phage display methods, SPR biosensors provide the kinetic data required to determine the extent to which an interaction takes place. Paired with site-directed mutagenesis and X-ray crystallography, SPR can help identify and validate key residues or motifs involved in binding; SPR data can distinguish the components of the binding interface that affect recognition and formation from those that maintain stability (Reichmann et al. 2005). Finally, with techniques used to identify and characterize protein complexes and cascades, SPR optical biosensors can provide data on the formation and stabilization of protein complexes consisting of multiple interaction partners (Spirin and Mirny 2003). Analyzing protein interactions under multiple conditions and among multiple interaction partners, however, requires an SPR optical biosensor capable of processing multiple samples in parallel while still yielding high-quality data.

The ProteOn XPR36 Protein Interaction Array System

The ProteOn XPR36 system is an SPR optical biosensor capable of simultaneous measurement of 36 individual molecular interactions. It integrates a high-efficiency microfluidics system with a high-sensitivity optical system to generate data over a unique 6 x 6 interaction array for the analysis of up to six ligands with up to six analytes.

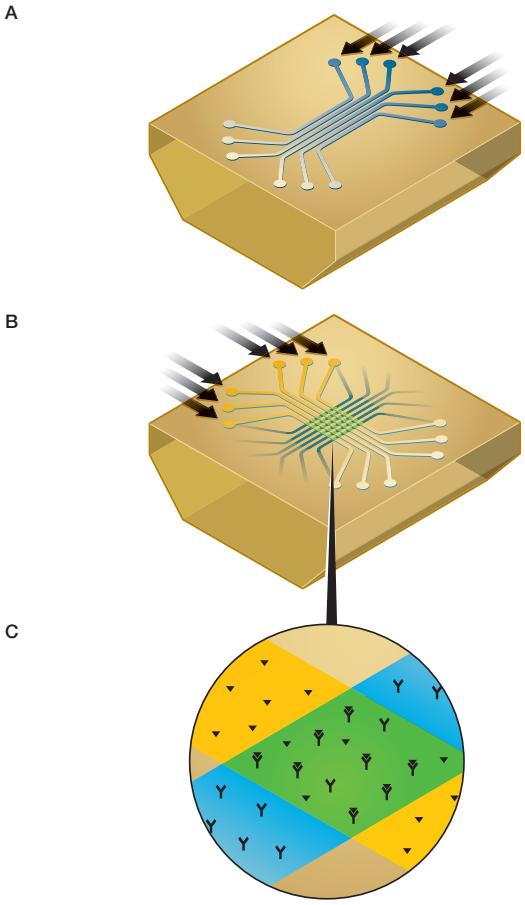

Fig. 2. Generation of the 6 x 6 ligand-analyte interaction array. A, six ligands are immobilized in six parallel ligand channels; **B**, six analyte samples are injected into six analyte channels orthogonal to the six ligand channels; **C**, detail of a single ligand-analyte interaction spot (green) showing the positions of the two interspot references (yellow).

A 6 x 6 Interaction Array Coupled With Efficient Fluidics

The 6 x 6 interaction array is generated by the centerpiece of the fluidics system, the multichannel module (MCM). The MCM forms six channels on the ProteOn sensor chip surface, and up to six different ligand samples can be immobilized in each of the channels. By rotating the MCM, a second set of channels is formed orthogonal to the first, creating a crisscross pattern of two sets of orthogonal flow channels (Figure 2). Up to six analyte samples can then be injected in parallel into this second set of channels. The response at each interaction spot is then detected, generating 36 sensorgrams corresponding to six analytes interacting with each of the six ligands. The associated fluidics ensure a smooth, constant flow of sample and buffer fluids for accurate measurement of binding kinetics.

Innovative Optics

The ProteOn XPR36 system also features an optics system capable of producing a high-quality response over the entire 36-element array. A synchronized sequential scanning illumination and imaging system detects the SPR response as the illumination passes through the critical angle (see sidebar on the previous page). The optical system has the additional advantage of scanning electronically with no moving parts. The complete SPR curve of intensity versus angle

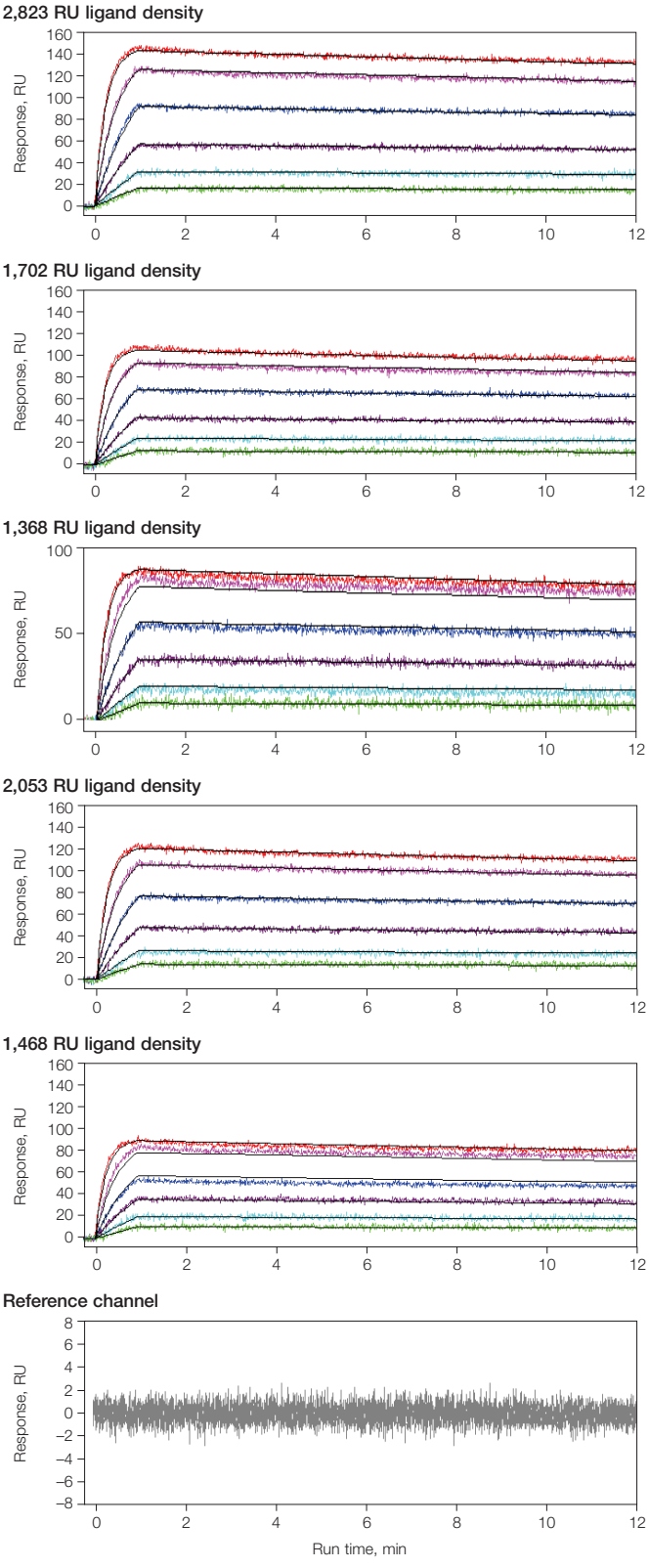

Fig. 3. One-shot kinetics for the IL-2 cytokine/IL-2 antibody interaction. Each set of six sensorgrams displays the responses from the six IL-2 cytokine concentrations interacting with one immobilization level of IL-2 antibody. Sensorgrams are shown for the five levels of IL-2 antibody immobilization (ligand density) and the reference channel. Black lines represent the global fit of the sensorgrams to a 1:1 kinetic interaction model.

Experimental Design Using the ProteOn XPR36 Protein Interaction Array System

The innovative crisscross microfluidic design of the ProteOn XPR36 system easily and rapidly performs a multitude of experiments.

One-Shot Kinetics
This technique permits acquisition of a complete kinetic profile of six analytes with six ligands. The automated injection of six analyte concentrations over a single ligand concentration, or six analyte concentrations over six ligand concentrations, permits expanded statistical inference and acceleration of experimental results (see example below).

Step 1. Immobilize IL-2 antibody. (Immobilization levels varied in each channel.)

EDC/sulfo-NHS (1x), IL-2 antibody, ethanolamine HCl
EDC/sulfo-NHS (0.5x), IL-2 antibody, ethanolamine HCl
EDC/sulfo-NHS (0.25x), IL-2 antibody, ethanolamine HCl
EDC/sulfo-NHS (0.125x), IL-2 antibody, ethanolamine HCl
EDC/sulfo-NHS (0.0625x), IL-2 antibody, ethanolamine HCl
Reference channel (PBS/Tween only)

Step 2. Analyze binding of cytokine IL-2.
(Cytokine concentration varied in each channel.)

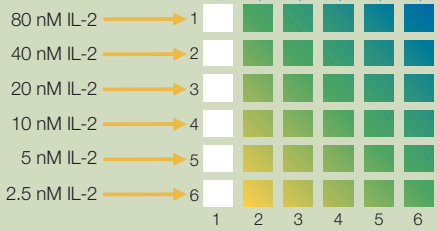

Analysis of Multiple Protein Interactions
Numerous life science applications require coordinated investigation of multiple interaction events between groups of closely related proteins and variants of a single protein.
- Efficiently immobilize up to 6 different ligands in one immobilization step, then sequentially analyze various analytes in successive binding steps
- Rapidly investigate complex interactions between several groups of closely related proteins
- Screen focused libraries against a panel of structurally similar targets, identifying the basis of binding specificity
- Map pharmacologically crucial details of the protein interfaces and binding sites of multiple mutant proteins, oligonucleotides, and peptide sequence variations

Testing of Multiple Conditions
A great advantage of the ProteOn XPR36 system is that multiple results are simultaneously obtained and instantly seen in the context of other conditions.
- Rapidly and accurately acquire kinetic, thermodynamic, specificity, and affinity data in one experiment of 36 separate interactions — all with the sensitivity of SPR technology
- Determine pH and salt effects on binding interaction and complex formation
- Perform competitive binding assays with concentration series of multiple analytes and competitors in parallel

Antibody Characterization
- Analyze, compare, and cross-reference up to 60 samples per hour in hybridoma screening and immunogenicity testing
- Obtain a complete epitope mapping and interaction matrix among a panel of 6 antibodies and 6 antigens — in a single experiment

of illumination is measured at each point on the sensor chip, and the shift of the SPR angle is determined accurately and independently for each point in the chip surface image.

Interspot References — Maximizing Throughput and Flexibility

The 6 x 6 array and microfluidics of the ProteOn XPR36 system provide efficient parallel processing of multiple samples, which is further enhanced by another innovation: the ability to measure the SPR response of 42 interspot references. Interspot references are regions on the sensor chip situated between the flow channels and adjacent to both sides of every interaction spot in the direction of analyte flow (Figure 2). During ligand immobilization, these interspot references are not exposed to activation or ligand solutions; during analyte binding, however, the interspot references are exposed to analyte flow. Because interspot references do not have bound ligand, they can be used in place of a reference channel. This feature permits all 6 x 6 microchannels to be used for interaction analysis, maximizing throughput and flexibility in experimental design (Bronner et al. 2006).

One-Shot Kinetics

The parallel processing capability of the ProteOn XPR36 system is ideally suited for the quick and efficient analysis of multiple protein interactions. An innovative technique termed "one-shot kinetics" achieves a robust kinetic analysis of an analyte concentration series without need for regeneration between samples (Figure 3; Bronner et al. 2006). Because multiple conditions can be tested in parallel, the process of optimizing the protocols for immobilization and binding reactions can be handled quickly and efficiently, and the high sample throughput of the ProteOn XPR36 system can then be applied to screening and comparative analysis of multiple samples, such as those encountered in hybridoma screening and immunogenicity testing (see the sidebar above and the articles on pages 22 and 25 for other examples of applications).

Conclusions

To fully understand the role of a protein, it is important to move beyond analysis of its expression patterns and identify the potential interactions of that protein with other biomolecules, determine the extent to which these interactions take place, and analyze their consequences on cellular function. Deciphering the character and extent of protein interactions unlocks the dynamics of virtually every cellular process. From protein interfaces to multiunit complexes and cascades, the ProteOn XPR36 system provides the high-quality data needed to decipher the fundamental interactions underlying protein function. The integrated 6 x 6 design of the system makes it a versatile tool that augments other protein analysis techniques for a wide variety of applications.

References

Bronner V et al., Rapid and efficient determination of kinetic rate constants using the ProteOn XPR36 protein interaction system, Bio-Rad bulletin 3172 (2006)

Reichmann D et al., The modular architecture of protein-protein binding interfaces, Proc Natl Acad Sci USA 102, 57–62 (2005)

Rich RL and Myszka DG, Survey of the year 2004 commercial optical biosensor literature, J Mol Recognit 18, 431–478 (2005)

Spirin V and Mirny L, Protein complexes and functional modules in molecular networks, Proc Natl Acad Sci USA 100, 12123–12128 (2003)

Analysis of Multiple Protein-Protein Interactions Using the ProteOn™ XPR36 Protein Interaction Array System

Vered Bronner,[1] Tsafrir Bravman,[1] Ariel Notcovich,[1] Dana Reichmann,[2] Gideon Schreiber,[2] and Kobi Lavie[1]
[1] Bio-Rad Laboratories Inc., Gutwirth Park, Technion, Haifa 32000, Israel
[2] Department of Biological Chemistry, Weizmann Institute of Science, Rehovot 76100, Israel

Introduction

Many biological systems require analysis of multiple protein-protein interactions to further the understanding of their function. One example of such an analysis is the investigation of the relative contributions of specific protein substructures and residues to the binding interface between TEM1 β-lactamase (TEM1) and the β-lactamase inhibitor protein (BLIP) (Figure 1) (Albeck and Schreiber 1999). TEM1 β-lactamase is one of over 200 different β-lactamases found in nature. These versatile enzymes are present in both gram-positive and gram-negative bacteria, and are the principal mechanism of resistance to antibiotics. BLIP is a secreted protein from the soil bacterium *Streptomyces clavuligerus* that inhibits a wide range of β-lactamases.

Mutated TEM1 residues were used to analyze the consequences of mutations on the binding energetics of the protein interface. Just as the change in free energy of binding between a mutant and wild-type protein indicates the relative energetic contribution of each residue to the total binding energy, changing multiple residues in concert permits the extent of cooperativity among residues to be examined. In this tech note we report on the kinetic analysis of the binding interactions of five TEM1 mutant proteins with BLIP as a model for constructing a high-resolution picture of the noncovalent interactions within the TEM1/BLIP binding interface. Through kinetic analysis, the relative change in free energy (ΔΔG) due to a mutation can be determined by comparing the affinities of binding with ($K_{A,\,mut}$) and without ($K_{A,\,wt}$) the mutation (Albeck and Schreiber 1999). Central to this analysis was the fast and accurate "one-shot kinetics" capability of the ProteOn XPR36 protein interaction array system (Bronner et al. 2006a). The ProteOn XPR36 surface plasmon resonance (SPR) optical biosensor incorporates a 6 x 6 microchannel module and an interaction array sensor chip for analysis of up to 36 protein interactions in a single, rapid experiment.

For a more complete description of the scope of the interactions measured, the methods used to derive binding energetics from kinetic constants, and a detailed analysis of the architecture of the TEM1/BLIP interface made possible by this experimental design, see Albeck and Schreiber (1999), Reichmann et al. (2005), and Bronner et al. (2006b).

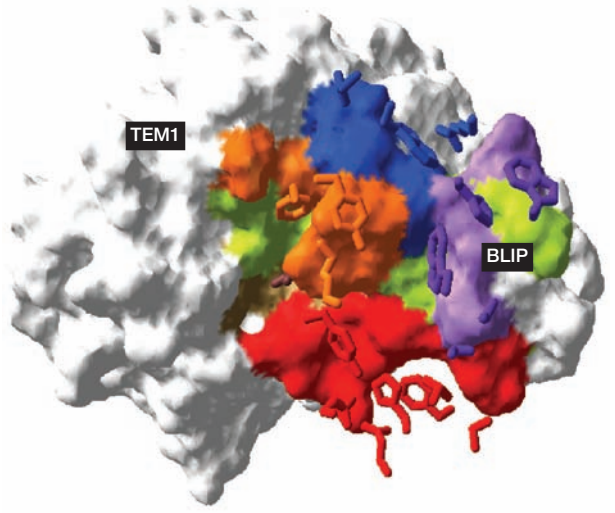

Fig. 1. Space-filling model of the binding interface between TEM1 and BLIP. The binding interface was resolved into five distinct modules (shown in color), with each module consisting of the noncovalent interactions of corresponding residues on each protein. See Reichmann et al. (2005) for details.

Methods

Instrumentation, Samples, and Reagents

The experiment was performed using the ProteOn XPR36 protein interaction array system, with one ProteOn GLC sensor chip, at 25°C. The protein expression and purification procedures used to prepare TEM1 (29 kD) mutant protein and wild-type BLIP (17.5 kD) samples are described by Albeck and Schreiber (1999). The five TEM1 mutants used were R243A/S235A, R243A/S130A, S130A/S235A, K234A, and E104A. ProteOn phosphate buffered saline with 0.005% Tween 20, pH 7.4 (PBS/Tween) was used as running buffer.

Sensorgram Analysis

A set of 36 sensorgrams was generated during a single injection step of the six BLIP samples and grouped into six sets of six. Each sensorgram set was processed for baseline alignment and reference channel subtraction.

Determination of Kinetic Rate Constants

Kinetic analysis was performed by globally fitting curves describing a simple 1:1 bimolecular reaction model to each set of six sensorgrams to obtain the association rate constant, k_a, and dissociation rate constant, k_d, from which the equilibrium dissociation constant, K_D, was calculated from the relationship $K_D = k_d/k_a$.

Protein-Protein Interaction Analysis

For immobilization of the five TEM1 mutant proteins, five of the six ligand channel surfaces were activated by injection of the amine coupling reagents 1-ethyl-3-(3-dimethylaminopropyl) carbodiimide hydrochloride (EDC, 100 mM) and N-hydroxy-sulfosuccinimide (sulfo-NHS, 25 mM) (components of the ProteOn amine coupling kit).

A 200 µl sample of each of the five TEM1 mutant proteins (2 µM, prepared in sodium acetate buffer, pH 4.0) and a buffer sample were injected at a flow rate of 30 µl/min in one injection cycle. To deactivate remaining carboxyl groups in the five channels, 1 M ethanolamine HCl, pH 8.5 (ProteOn amine coupling kit) was then injected. A sample of running buffer was included in each step for injection into the sixth channel, which was used as a reference channel.

Next, a serial dilution of BLIP samples was prepared at 600, 300, 150, 75, 37.5, and 18.75 nM in PBS/Tween, pH 7.4. Samples (150 µl) of each concentration were injected into the six analyte channels orthogonal to the TEM1 ligand channels at a flow rate of 100 µl/min, generating the 36-element interaction array. The binding kinetics for the interactions of each of the five TEM1 mutant proteins with BLIP were then rapidly and accurately obtained in "one shot" on a single chip (Bronner et al. 2006a).

Results and Discussion

Of the six sets of sensorgrams obtained, five corresponded to the interaction of the six BLIP concentrations with one of the TEM1 mutant proteins (Figure 2), and one set to the reference channel (not shown). The kinetic constants for each TEM1 mutant protein with BLIP are shown in Table 1. Note that the affinities of the interactions varied significantly, indicating the relative contributions of the mutated residues to the binding interface.

Table 1. One-shot kinetic values for the interaction of BLIP and TEM1 mutants.

TEM1 Mutant	k_a ($M^{-1}sec^{-1}$)	k_d (sec^{-1})	K_D (nM)
R243A/S235A	1.51×10^4	5.09×10^{-4}	33.8
R243A/S130A	1.27×10^4	1.24×10^{-3}	97.6
S130A/S235A	3.10×10^4	9.33×10^{-4}	30.1
K234A	2.01×10^4	8.50×10^{-4}	42.3
E104A	1.70×10^5	7.40×10^{-3}	43.5

While a detailed interpretation of these results requires knowledge of the placement of each residue within the interface (as may be obtained from structural analysis by crystallography), and also supplemental kinetic data obtained from analysis of the interactions between the wild-type protein forms (not shown) and other mutants for proper evaluation of the free energy changes induced by each mutant protein, a few conclusions may be reached from the limited data presented here.

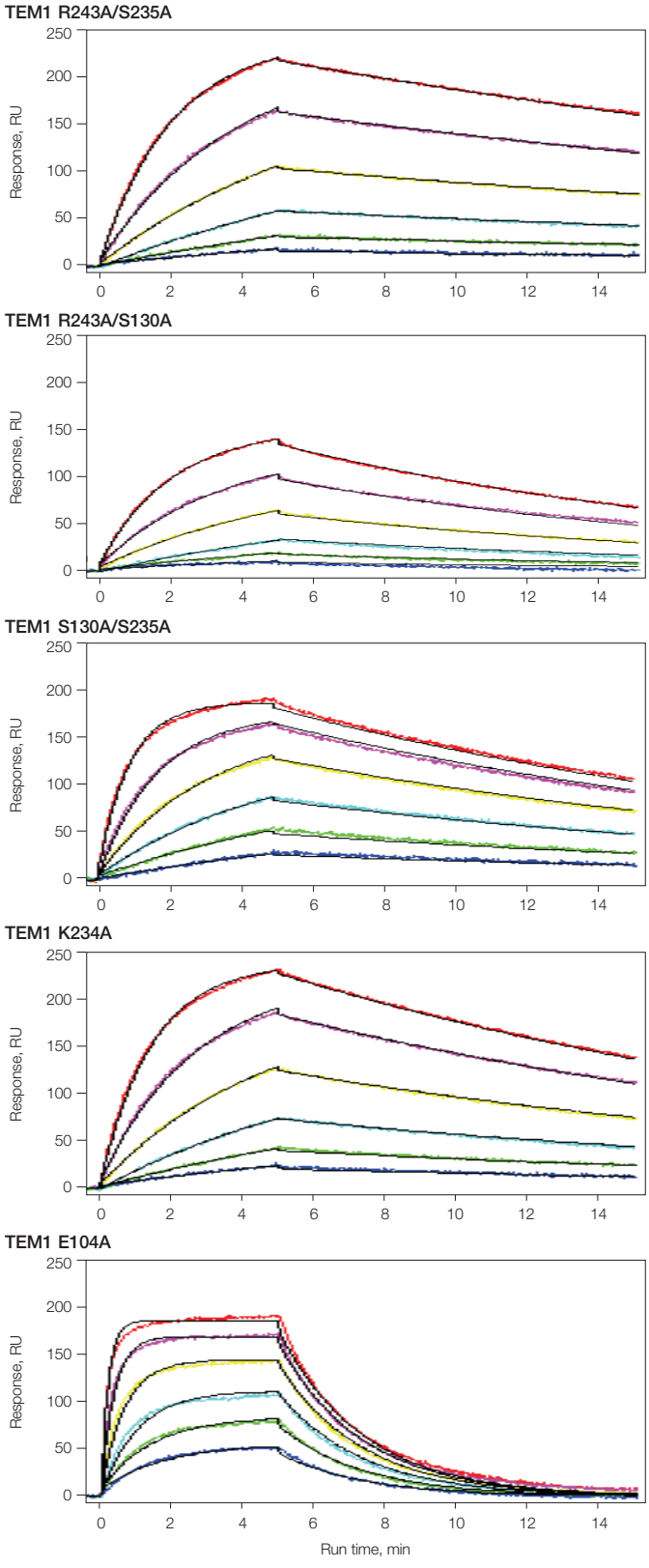

Fig. 2. One-shot kinetics for the interactions between BLIP and five TEM1 mutant proteins. Each set of six sensorgrams displays the responses from the six BLIP analyte concentrations (—, 600 nM; —, 300 nM; —, 150 nM; —, 75 nM; —, 37.5 nM; —, 18.75 nM) interacting with one (2 µM) TEM1 mutant protein ligand. Black lines represent the global fit of the sensorgrams to a 1:1 kinetic interaction model. See Table 1 for the kinetic constants derived from these data.

Each of the TEM1 mutations analyzed slightly weakens the TEM1-BLIP interface. The lower affinity with BLIP is indicated by the reduced association and enhanced dissociation rate constants of the TEM1 mutant proteins relative to TEM1 wild type. For example, removal of positively charged residues from TEM1, as represented by TEM1 K234A (lysine to alanine), results in a significant reduction of the association rate constant due to lessened electrostatic attraction with a corresponding aspartic acid residue on BLIP during the association phase. However, removal of a negative charge from TEM1 causes little change in the association rate constant, as represented by TEM1 E104A (glutamic acid to alanine).

The contribution of each mutated residue to the stabilization of the complex can be seen by the effect on the dissociation rate constants. The observed change in dissociation rate constants depends on the alteration of the specific interactions that each mutated residue has with its few neighboring residues in the interface. Note that the destabilization induced by TEM1 E104A is significantly greater than that due to the other mutations, as this residue interacts deep within the interface, although each mutation increases the dissociation rate relative to the wild type to some extent.

Conclusions

The rapid acquisition of accurate protein interaction data is a vital need in the investigation of many biological systems. The rapidly expanding field of proteomics, for example, demands reproducible, robust, high-performance methods to supplement traditional technology in the interrogation of the immense network of protein interactions in a cell. The ProteOn XPR36 protein interaction array system rapidly generates a 6 x 6 interaction array between six ligands and six analytes, and enhances studies of multiple protein interactions designed to map protein interfaces and resolve protein complexes. The example described here of an experimental design for analysis of multiple protein-protein interactions serves as a model for protocol development for the ProteOn XPR36 system.

References

Albeck S and Schreiber G, Biophysical characterization of the interaction of the β-lactamase TEM-1 with its protein inhibitor BLIP, Biochemistry 38, 11–21 (1999)

Bronner V et al., Rapid and efficient determination of kinetic rate constants using the ProteOn XPR36 protein interaction array system, Bio-Rad bulletin 3172 (2006a)

Bronner V et al., Mechanisms of protein-protein binding: double mutant cycle analysis, Bio-Rad bulletin 5358 (2006b)

Reichmann D et al., The modular architecture of protein-protein binding interfaces, Proc Natl Acad Sci USA 102, 57–62 (2005)

For additional copies of this article, request bulletin 5368.

Rapid and Detailed Analysis of Multiple Antigen-Antibody Pairs Using the ProteOn™ XPR36 Protein Interaction Array System

Vered Bronner, Tsafrir Bravman, and Kobi Lavie, Bio-Rad Laboratories, Inc., Gutwirth Park, Technion, Haifa 32000, Israel

Introduction

The ProteOn XPR36 protein interaction array system is a surface plasmon resonance (SPR) biosensor with a microchannel module and interaction array sensor chip for analysis of up to 36 protein interactions in a single injection step. The capability of the ProteOn XPR36 system to rapidly generate a 6 x 6 interaction array between six ligands and six analytes greatly increases the throughput, flexibility, and versatility of experimental design for a wide range of biomolecular interaction studies (Figure 1). Additional details on this array-format system are provided in Bronner et al. (2006).

We describe here the rapid and detailed kinetic analyses of four antigen-antibody interactions. Briefly, the interaction of each antibody (ligand) with a concentration series of its respective antigen (analyte) was analyzed in a sequence of a single immobilization cycle followed by four analyte injection cycles. Four different antibodies and a nonreactive negative control protein were immobilized in five parallel ligand channels on a single ProteOn sensor chip; the sixth ligand channel was left blank for use as a reference channel. For each antibody, a concentration series of antigen samples (six samples spanning a wide concentration range) was then injected into the set of six parallel analyte channels orthogonal to the ligand channels. The ligand channels were then regenerated for analysis of the next antigen concentration series, until all four antigen-antibody interactions were analyzed.

Each of the four antigen injections produced a set of 36 sensorgrams. These contained data not only on the interaction of an antigen concentration series with its respective antibody, but also on its interaction with each of the three other antibodies, the negative control protein, and the reference channel. Thus, data sufficient to perform a detailed kinetic analysis of each antigen-antibody interaction — as well as a determination of any potential cross-reactivity among the antigens and antibodies — were obtained in a minimal number of injection steps.

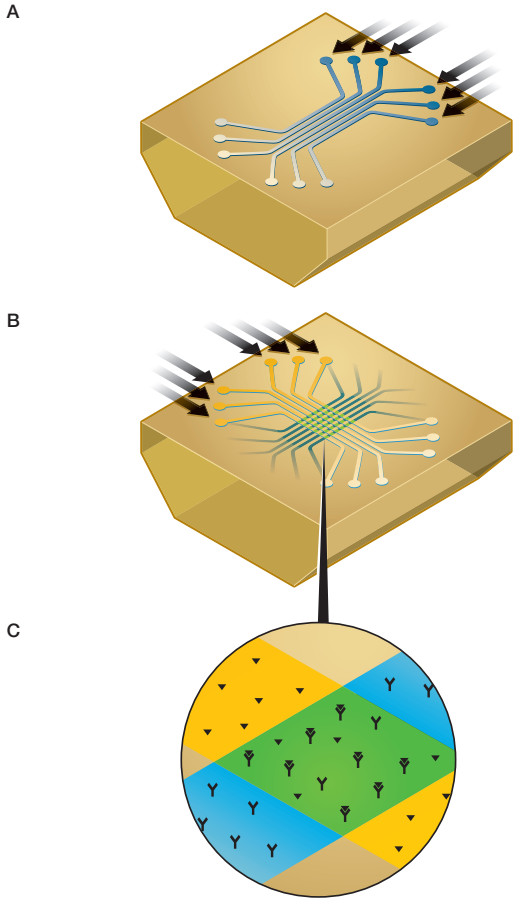

Fig. 1. Generation of the 6 x 6 ligand-analyte interaction array. A, six ligands are immobilized in six parallel ligand channels; **B**, six analyte samples are injected into six analyte channels orthogonal to the six ligand channels; **C**, detail of a single ligand-analyte interaction spot (green) showing the positions of the two interspot references (yellow).

Methods

Instrumentation and Reagents

Experiments were performed using the ProteOn XPR36 protein interaction array system and one ProteOn GLC sensor chip. ProteOn phosphate buffered saline with 0.005% Tween 20, pH 7.4 (PBS/Tween) was used as running buffer throughout the experiments, and all experiments were performed at 25°C.

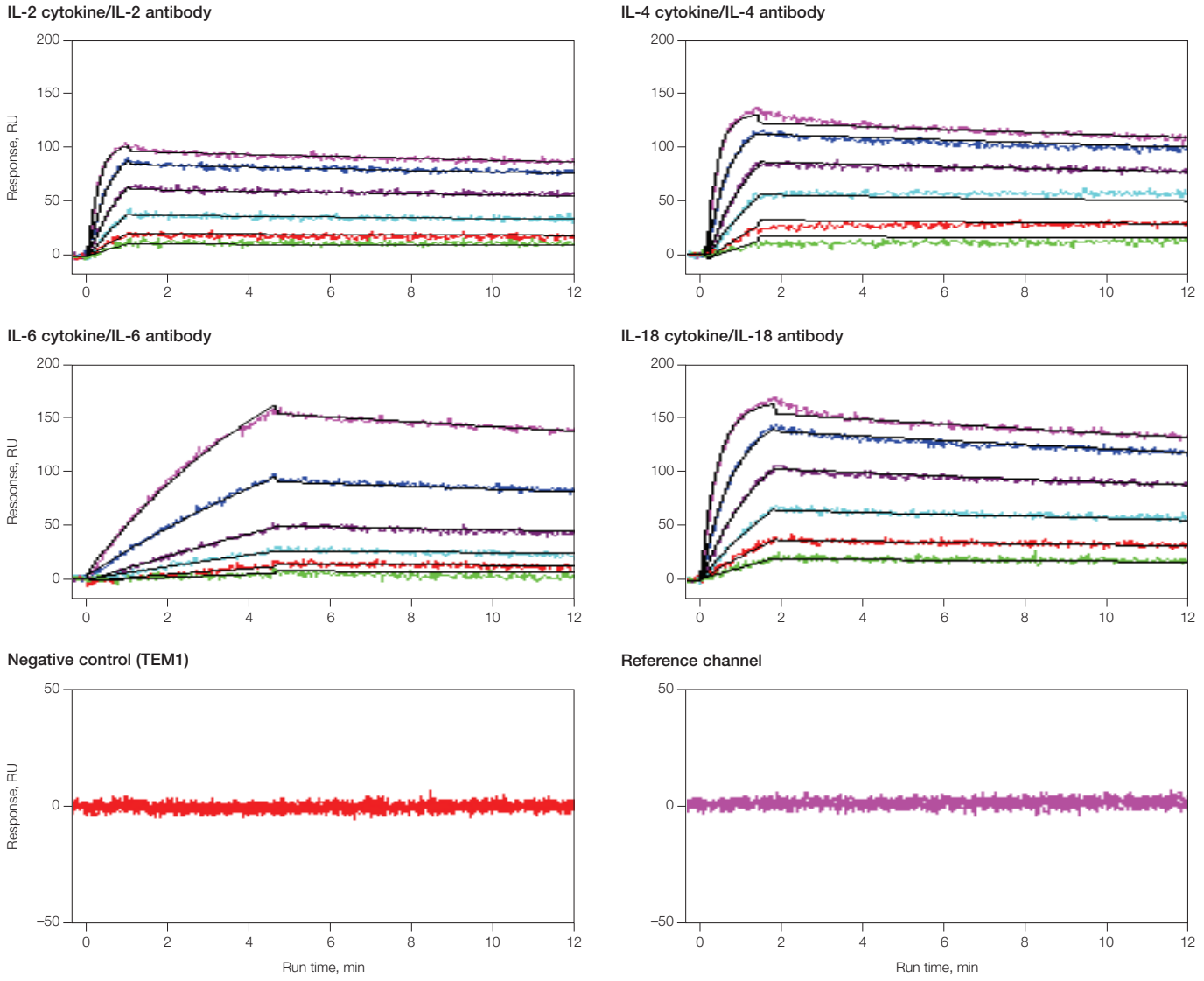

Fig. 2. Kinetic analysis of four antigen-antibody interactions. Shown are the four sets of sensorgrams generated for each specific antibody-antigen pair, as well as sensorgrams from the interaction of the IL-2 concentration series with the negative control and reference channel. The interactions of the four cytokines are shown from the highest cytokine concentrations (top traces) to the lowest concentrations (bottom traces). Black lines represent the global fit of the sensorgrams to a 1:1 interaction kinetic model. See Table 1 for the kinetic constants derived from these data.

Immobilization of Antibodies

Using the parallel sample processing capability of the ProteOn XPR36 system, the immobilization cycle of the four antibodies and negative control protein was accomplished in only three injection steps for surface activation, ligand coupling, and surface deactivation.

First, the ProteOn GLC sensor chip surface was activated in five of the six ligand channels by injection of the amine coupling reagents 1-ethyl-3-(3-dimethylaminopropyl)carbodiimide hydrochloride (EDC, 100 mM) and N-hydroxysulfosuccinimide (sulfo-NHS, 25 mM) (components of the ProteOn amine coupling kit). The sixth channel was not modified and served as a reference channel.

Next, the four antibodies were diluted to the following concentrations in 10 mM ProteOn acetate buffer, pH 4.5: IL-2 antibody, 25 µg/ml (mouse anti-human IL-2, ProteOn IL-2/IL-2 antibody pair); IL-4 antibody, 50 µg/ml (mouse anti-human IL-4, Biosource International); IL-6 antibody, 12.5 µg/ml (mouse anti-rat IL-6, BD Biosciences Pharmingen); and IL-18 antibody, 12.5 µg/ml (hamster anti-mouse, Medical and Biological Laboratories Co., Ltd.). The four antibody samples (180 µl) and a nonreactive protein (TEM1 β-lactamase, 180 µl) were injected into the five activated ligand channels at a flow rate of 30 µl/min for immobilization. Lastly, to deactivate remaining carboxyl groups, 1 M ethanolamine HCl, pH 8.5 (ProteOn amine coupling kit) was then injected into the five activated channels. A buffer sample was included in each step for injection into the reference channel.

Table 1. Kinetic constants for four antigen-antibody interactions. The equilibrium dissociation constant, K_D, was calculated from k_d/k_a.

	Antibody (Ligand)	Antigen (Analyte)			
Channel	Ligand Density (RU)	k_a ($M^{-1}sec^{-1}$)	k_d (sec^{-1})	K_D (M)	R_{max} (RU)
(1) IL-2	1,470 ± 2.65%	8.68×10^5	1.84×10^{-4}	2.12×10^{-10}	112
(2) IL-4	1,097 ± 4.64%	2.38×10^6	2.21×10^{-4}	9.29×10^{-11}	139
(3) IL-6	1,530 ± 1.86%	3.72×10^4	2.93×10^{-4}	7.89×10^{-9}	336
(4) IL-18	2,588 ± 1.28%	6.15×10^5	2.33×10^{-4}	3.78×10^{-10}	175

Antigen Interaction Analysis

Antigen samples were all prepared by serial dilution in PBS/Tween. Human IL-2 cytokine (ProteOn IL-2/IL-2 antibody pair) and rat IL-6 cytokine (BD Biosciences Pharmingen) samples were prepared at concentrations of 80, 40, 20, 10, 5, and 2.5 nM. Human IL-4 cytokine (Research Diagnostics, Inc.) samples were prepared at 32, 16, 8, 4, 2, and 1 nM, and mouse IL-18 cytokine (Medical and Biological Laboratories Co., Ltd.) samples at 60, 30, 15, 7.5, 3.8, and 1.9 nM.

Each concentration series of antigen was injected into the six analyte channels orthogonal to the ligand channels at a flow rate of 100 µl/min. The durations of these injections were 60 sec for 100 µl of IL-2 or IL-4, 120 sec for 200 µl of 1L-18, and 240 sec for 400 µl of IL-6. The durations of the IL-6 and IL-18 injections were increased to produce sufficient curvature in the association phase of the sensorgrams for kinetic analysis. The ligand channels were regenerated between injections of each antigen concentration series by a short pulse (30 µl) of 0.85% phosphoric acid.

Sensorgram Analysis

The 36 sensorgrams produced from each antigen injection were grouped into six sets of six, with each set corresponding to the interaction of an antigen concentration series with the four immobilized antibodies, negative control protein, and reference channel. The sensorgrams were processed for baseline alignment and referencing.

In addition to the reference channel, interspot references were used for background subtraction. Interspot references are exposed to analyte flow but do not have bound ligand, and so can be used in place of a reference channel (Bronner et al. 2006). When the response of each interaction spot was corrected by the average response from its two adjacent interspot references, the results were identical to those obtained using the reference channel (Figure 2).

Results and Discussion

The four sets of six sensorgrams were globally fit to a 1:1 bimolecular interaction model (Figure 2). The adjustable kinetic parameters for association (k_a), dissociation (k_d), and R_{max} for each interaction were derived from the fitted curves (Table 1).

The coefficients of variation of the kinetic constants obtained from samples analyzed at different times were in the range of 10%. The percent differences for ligand density in Table 1 were computed from the six interaction spots along a single ligand channel.

The kinetic properties of the different antigen-antibody interactions are readily compared. Table 1 summarizes the association and dissociation rates obtained from the fitted curves for each of the four antigen-antibody interactions, and the calculated equilibrium dissociation constant (K_D). The slower association rate (k_a) of IL-6/IL-6 antibody binding (3.72×10^4 $M^{-1}sec^{-1}$) was notable in comparison to the association rates of the other antigen-antibody pairs ($0.6–2.4 \times 10^6$ $M^{-1}sec^{-1}$). The dissociation constants (k_d) were similar for all pairs ($1.84–2.93 \times 10^{-4}$ sec^{-1}). This comparison of kinetic constants indicates a difference of 2 orders of magnitude in the equilibrium dissociation constants of IL-6 ($K_D = 7.89 \times 10^{-9}$ M) and IL-4 ($K_D = 9.29 \times 10^{-11}$ M).

In this experiment, no interaction between antigens and unrelated antibodies was detected, indicating no cross-reactivity (data not shown).

Conclusions

The ProteOn XPR36 protein interaction array system is well-suited for experimental designs in which a number of interacting protein pairs are to be analyzed and compared. Data can be rapidly obtained for protein interface characterization, affinity ranking, and epitope mapping of antibodies, as well as for selecting lead compounds in drug development.

The capability of the ProteOn XPR36 system to rapidly perform a detailed kinetic analysis of multiple protein-protein interactions in a 6 x 6 interaction array format is especially useful for antibody development and characterization. Here the kinetic rate constants were determined for four antigen-antibody pairs using just one ProteOn sensor chip and a minimum number of injection cycles. This throughput, together with the fact that the interactions between each antigen and the other immobilized antibodies are also measured (which offers information on cross-reactivity), makes the ProteOn XPR36 system a powerful tool for protein interaction analysis.

Reference

Bronner V et al., Rapid and efficient determination of kinetic rate constants using the ProteOn XPR36 protein interaction array system, Bio-Rad bulletin 3172 (2006)

For additional copies of this article, request bulletin 5360.

Using the Molecular Imager® PharosFX™ System to Image Arrays Printed With the BioOdyssey™ Calligrapher™ MiniArrayer

Cathleen Karlak, Kevin McDonald, Theresa Redila-Flores, and Luis Ugozzoli, Bio-Rad Laboratories, Inc., Hercules, CA 94549 USA

Introduction

The BioOdyssey Calligrapher miniarrayer is designed to print arrays onto glass slides, into 96-well microplates, or onto membranes. Printing onto membranes or nitrocellulose-coated slides is particularly useful for proteomics research. Two-color laser scanners typically scan 1" x 3" slides and will not accommodate larger nitrocellulose formats. In this study, we investigated imaging both nitrocellulose membranes and FAST slides with the Molecular Imager PharosFX system.

The PharosFX system is designed specifically for complex imaging applications involving multiple fluorescence wavelengths in gels, blots, microplates, and macroarrays. It allows multicolor detection of a wide range of fluorophores via direct laser excitation, high excitation efficiency, and precise spectral assignment. The system's excitation/emission filter combinations are designed to maximize the signal-to-noise ratio (SNR) and thus increase sensitivity.

Here, we examine the ability of the PharosFX system to scan microarrays on nitrocellulose membranes and FAST slides, a glass-supported nitrocellulose surface fabricated by the Calligrapher miniarrayer. We demonstrate that the PharosFX system performs with the same sensitivity as a two-color microarray scanner when used with a nitrocellulose substrate arrayed with an adequate spot size.

Methods

For each test, arrays were printed with the BioOdyssey Calligrapher miniarrayer equipped with two pins, either Stealth SMP3 or SMP11 microarray spotting pins (TeleChem International, Inc.). Substrates included 0.2 µm pore nitrocellulose membranes (Whatman Inc.) cut to fit into an OmniTray (Nalge Nunc International) or FAST slides (Whatman Inc.). Oligonucleotides labeled with one of three dyes, Alexa Fluor 546 (Integrated DNA Technologies, Inc.), Quasar570 (BioSearch Technologies, Inc.), or Cy3 (TriLink BioTechnologies, Inc.), were arrayed individually on the substrates. The dye-labeled oligonucleotides were suspended at 50 µM in 1x Bio-Rad printing buffer containing 200 ng/µl carrier salmon sperm DNA. A series of 2-fold serial dilutions was carried out to yield a final oligonucleotide concentration of 0.095 nM. The dilution series was spotted onto each substrate at least in triplicate. To print the larger spot size, the spot distance for the grid was adjusted to 1,600 µm by accessing the Advanced Grid of the Define Array Parameters feature (Figure 1).

After arraying, the substrates were dried for 30 min and then imaged with the PharosFX system using 532 nm excitation and 605 nm emission filters, with the gain set at 35% for the membrane and at 55% for the FAST slides. For comparison, the printed arrays were also imaged using a two-color microarray scanner. To image nitrocellulose membranes in the microarray scanner, membranes were cut to fit onto a glass slide, and secured with thin pieces of tape. At an SNR (background-adjusted signal divided by the standard deviation of the background signal) of 3, the limit of detection (LOD) for each substrate with each instrument was determined in fluorophores/µm^2. This value was calculated as: (volume deposited) x (concentration of oligo) x Avogadro's number/surface area of the spot. For FAST slides, we assumed that the volume deposited was 0.7 nl for SMP3 pins and 4.4 nl for SMP11 pins. For membranes, we assumed that 50 nl was deposited, based on printing 3–4 spots/dip.

Results and Discussion

We tested three dyes with similar spectral properties, Cy3, Alexa Fluor 546, and Quasar570, and found that each performed similarly (data not shown). All results shown in this report were obtained with Cy3. The rainbow images collected from the PharosFX are shown in Figure 2.

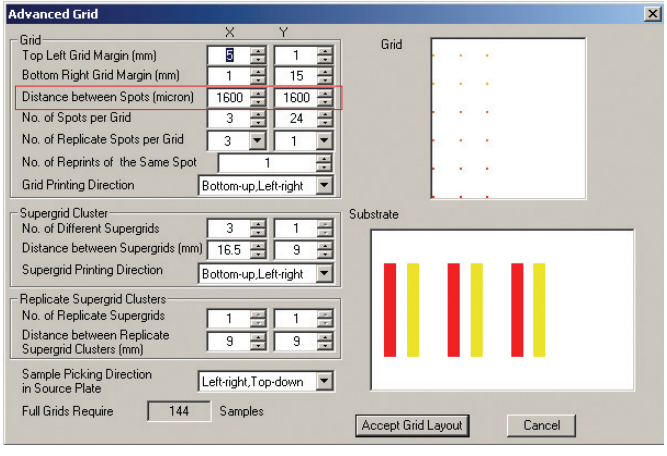

Fig. 1. Advanced Grid window displays the parameters used for printing nitrocellulose membranes using TeleChem SMP11 pins. The "Distance between Spots" has been set to 1,600 µm to account for wicking.

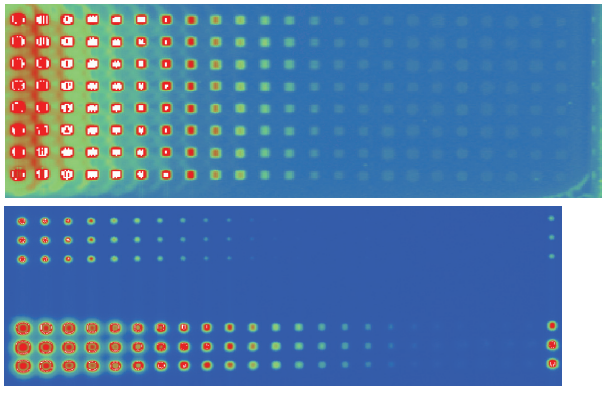

Fig. 2. Rainbow images of substrates containing Cy3-labeled oligonucleotide dilutions imaged with the PharosFX scanner. Top, FAST slide with 400 µm spots; bottom, nitrocellulose membrane (upper rows are 400 µm spots, lower rows are 800 µm). Spots were arrayed as described in the text.

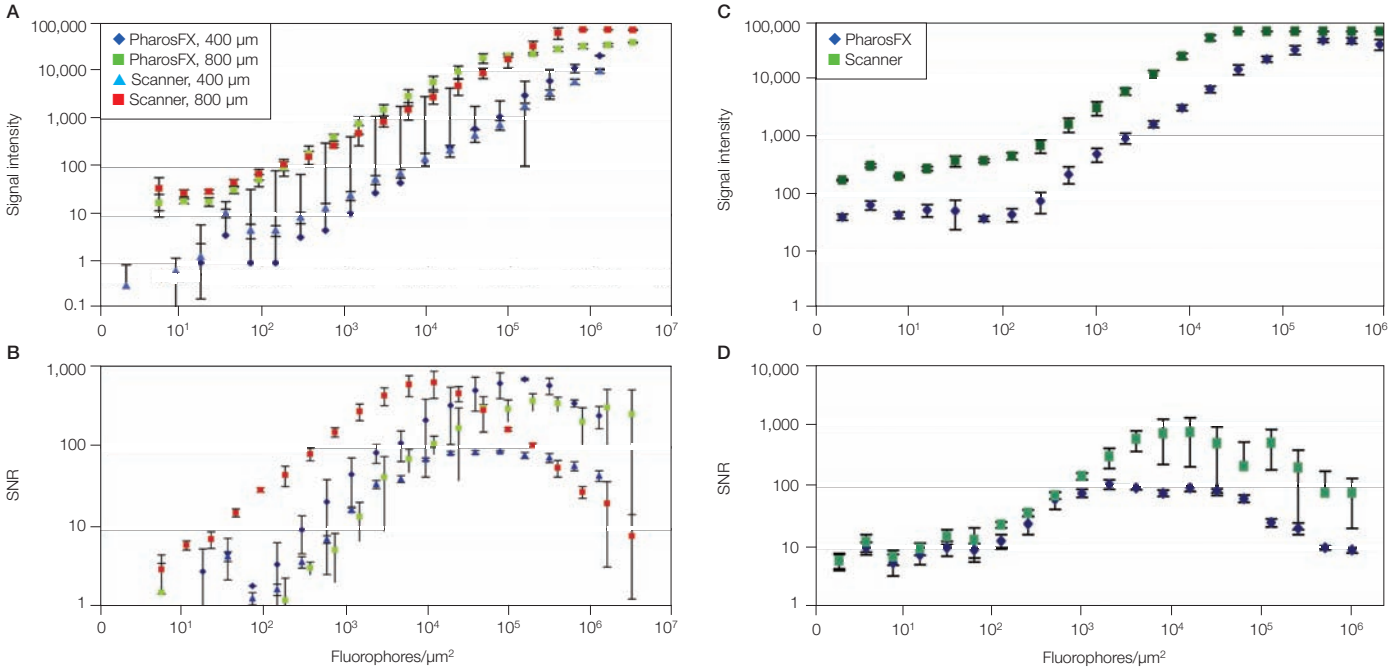

Fig. 3. Comparison of signal intensity and SNR of arrays measured using the PharosFX system and a two-color microarray scanner. A, signal intensity, and **B**, SNR for nitrocellulose membranes. Values are averages of three replicates. **C**, signal intensity, and **D**, SNR for FAST slides. Values are averages of eight replicates. SNR was calculated by dividing the background-corrected signal by the SD of the background. Error bars indicate SD. FAST slides show only one spot size, as described in text.

In general, for an imaging device to detect a spot, the spot must be composed of at least 50–100 pixels. Since the resolution of the PharosFX is 50 µm, it was expected that a spot size of at least 400 µm would be required to reliably detect the spots. This spot diameter was achieved on FAST slides using the SMP11 pin, and on nitrocellulose membranes using the SMP3 pin. The SMP11 pin printed an 800 µm spot diameter on nitrocellulose membrane. The diameters printed on nitrocellulose membrane were greater than on FAST slides due to sample wicking.

Figure 3 displays the signal intensity and SNR obtained with the PharosFX or the microarray scanner for each fluorophore concentration and each spot diameter on nitrocellulose membranes and FAST slides. We attribute the higher error rates seen with the nitrocellulose to its physical properties.

Equivalent signal intensity was obtained with either the PharosFX or the microarray scanner when imaging FAST slides printed with SMP11 pins. The larger spot sizes (400 µm) produced by the SMP11 pin yielded adequate data for the PharosFX to capture.

Likewise, equivalent signal intensity was obtained with either the PharosFX or the microarray scanner when analyzing imaged array data from nitrocellulose membranes printed with either the SMP3 or SMP11 pin. Data were obtained over approximately 5 orders of magnitude using either instrument for both substrates. However, larger spot sizes (800 µm) were necessary to yield acceptable data from both the PharosFX system and the laser scanner.

The SNR results showed similar trends for each instrument and each substrate (Figure 3B, D). The higher the SNR, the more reliably the instrument can differentiate a signal from background. The commonly accepted SNR value of 3 was used to determine the LOD data shown in Table 1. The larger spot diameter (800 µm) on the membrane was required to obtain an acceptable LOD of 6–10 fluorophores/µm^2.

Table 1. Comparison of limit of detection (LOD) obtained with different array substrates and imaging instruments at two spot diameters.

Substrate	Instrument	Pin Type	Spot Size (µm)	LOD
FAST slide	PharosFX system	SMP11	400	2–4 fluorophores/µm^2
	Microarray scanner	SMP11	400	2–4 fluorophores/µm^2
Nitrocellulose	PharosFX system	SMP3	400	300–600 fluorophores/µm^2
	Microarray scanner	SMP3	400	300–600 fluorophores/µm^2
	PharosFX system	SMP11	800	6–10 fluorophores/µm^2
	Microarray scanner	SMP11	800	6–10 fluorophores/µm^2

Conclusions

The BioOdyssey Calligrapher miniarrayer has the flexibility to print onto various substrates, including nitrocellulose membranes. We have demonstrated that the PharosFX system can accurately quantitate fluorescent arrays fabricated on nitrocellulose membranes or FAST slides when an appropriate spot size is printed. The values obtained with the PharosFX were consistent with those measured using a standard microarray scanner. While only data with a Cy3-labeled oligonucleotide are shown here, the PharosFX has multiple excitation lasers coupled with emission filters that allow detection of different fluorophores, a flexibility that allows scientists to perform various types of assays using arrays printed with the Calligrapher miniarrayer.

We have also demonstrated that imaging for the quantitation of arrays on nitrocellulose can be performed with a standard laser-based microarray scanner by simply affixing the membrane to a glass slide. These options should allow greater use of array technology in laboratories equipped with either type of scanner.

For additional copies of this article, request bulletin 5436.

Automated Three-Dimensional Purification Method for Histidine-Tagged Proteins Using the BioLogic DuoFlow Maximizer™ Chromatography System

Fang-Fang Wu and Roger Provost, Bio-Rad Laboratories, Inc., Hercules, CA 94547 USA

Introduction

Protein purification can involve challenging separations of complex mixtures that may not resolve target proteins in a single chromatographic step. Such cases may require the use of multidimensional chromatography. Multidimensional chromatography combines a series of columns, each employing different separation mechanisms, into a single separation scheme. Most common protein purification techniques can be incorporated into a multidimensional chromatography scheme, and such schemes provide great benefit for proteins purified on a routine basis. Typically, a multidimensional chromatographic scheme consists of an affinity purification step based on binding to a protein tag, such as multiple histidine (His) residues or glutathione-S-transferase (GST), followed by one or more additional resolution steps using ion exchange, size exclusion, or hydroxyapatite columns. To streamline the combination of such disparate chromatographic methods, an automated chromatography system with a flexible design and versatile control software is essential.

In this study, we describe an automated three-step (three-dimensional) chromatographic method for purification of a recombinant 100 kD His-tagged protein from a crude *E. coli* lysate. The method involved initial affinity capture of the tagged protein using Ni^{2+}-charged Profinity™ IMAC support, intermediate desalting with Bio-Gel® P-6DG desalting gel, and final purification on an UNO® Q1 anion exchange column. Using the high valve capacity provided by the BioLogic DuoFlow Maximizer chromatography system, we optimized the flow path with parallel connection of the three columns using one UV detector and one conductivity monitor (Figure 1).

Using the queuing feature of BioLogic DuoFlow™ software, the three-dimensional method was written as a series of individual one-dimensional method runs. The BioLogic DuoFlow multimodule hardware and software facilitated the routine running of this complex purification process, which required three columns and nine buffers, without operator attendance. This automated method yielded reliable, efficient His-tagged protein purification.

Methods

System Components and Buffers

The BioLogic DuoFlow Maximizer 20 chromatography system was used in this study. Components were connected to the F10 workstation and controller as illustrated in Figure 1 and included the following: three columns, a UV detector, a conductivity monitor, a BioFrac™ fraction collector, three AVR7-3 injection valves, two SV5-4 buffer select valves, two AVR9-8 stream-select valves, and two SV3T-2 valves, one for loop selection and the other for flow diversion. Nine buffers were used, and all were filtered, degassed, and connected to the SV5-4 valves as shown in Figure 1: A1, affinity equilibration buffer (50 mM potassium phosphate, 300 mM NaCl, pH 8.0); A2, affinity elution buffer (A1 buffer with 500 mM imidazole); A3, ion exchange buffer A (20 mM Bis-Tris, pH 6.0); A4, desalting buffer (20 mM Bis-Tris, pH 6.0); B1, ion exchange buffer B (20 mM Bis-Tris, 1 M NaCl, pH 6.0); B2, discharging buffer (50 mM EDTA, 300 mM NaCl, 50 mM potassium phosphate, pH 7.5); B3, charging buffer (100 mM $NiSO_4$, pH 4.0); B4, cleaning buffer (50 mM KOAc, 300 mM NaCl, pH 4.0).

Purification Protocol

The following columns were used: a 1 ml Tricorn column (0.5 x 5 cm) (GE Healthcare) manually packed with Ni^{2+}-charged Profinity IMAC support, a 10 ml Amicon column (1.2 x 8.8 cm) (Millipore) manually packed with Bio-Gel P-6DG desalting gel, and an UNO Q1 column (0.7 x 3.5 cm) prepacked with 1.3 ml anion exchange matrix.

Methods specific to each column type or step (described below) were created independently, linked using the queuing function of BioLogic DuoFlow 5.1 software, and executed sequentially. During the process, as a fraction containing the target 100 kD His-tagged protein eluted from one column, it was automatically transferred to the next column through an intermediate loop.

Affinity Capture — The Profinity IMAC column was equilibrated with 5–10 ml affinity equilibration buffer (A1) at a flow rate of 1 ml/min. Next, 1 ml crude *E. coli* lysate supernatant containing the 100 kD His-tagged protein was loaded on a 1 ml injection loop and injected through AVR7-3 injection valve 1 (Figure 1). The column was washed with 5 ml, or 5 column volumes (CV), of affinity equilibration buffer (A1) to remove host protein contaminants, the vast majority of which should not be retained by Profinity IMAC support. The 100 kD His-tagged protein was eluted with affinity elution buffer (A2) until all of it was removed. During elution, once the 100 kD protein peak was detected, the flow path was changed and directed the fraction containing the protein to AVR7-3 sample loop 2 (Figure 1). Finally, the column was washed with an additional 5 ml (5 CV) affinity elution buffer (A2) to eliminate residual proteins.

To regenerate the Profinity IMAC column for future runs, the column was stripped with 10 ml (10 CV) discharging buffer (B2) and then washed with 10 ml (10 CV) cleaning buffer (B4). The

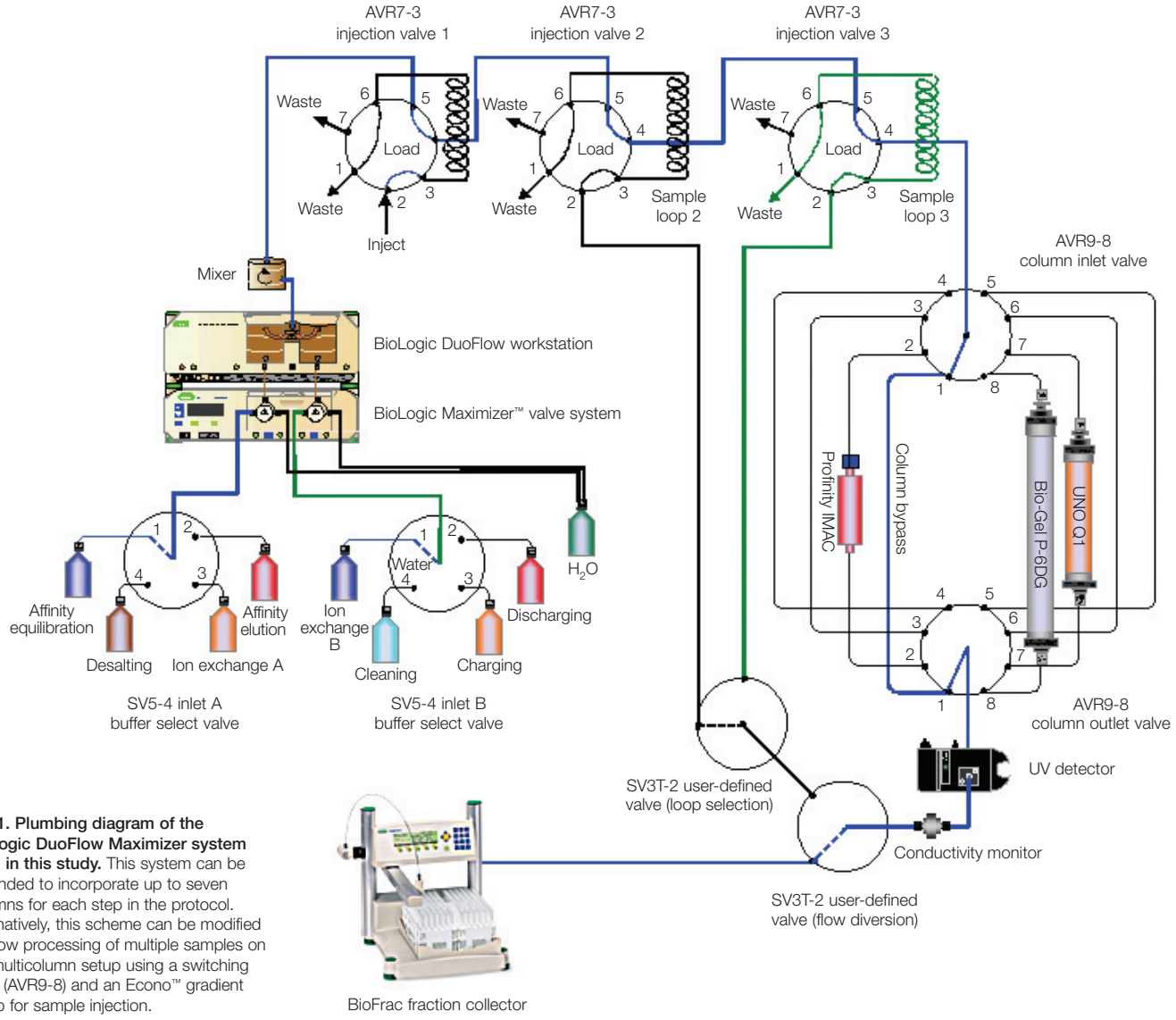

Fig. 1. Plumbing diagram of the BioLogic DuoFlow Maximizer system used in this study. This system can be expanded to incorporate up to seven columns for each step in the protocol. Alternatively, this scheme can be modified to allow processing of multiple samples on the multicolumn setup using a switching valve (AVR9-8) and an Econo™ gradient pump for sample injection.

column was recharged with 10 ml (10 CV) charging buffer (B3), washed with 10 ml (10 CV) cleaning buffer (B4), and then reequilibrated with 10 ml (10 CV) affinity equilibration buffer (A1).

Desalting — The 10 ml column containing Bio-Gel P-6DG desalting gel was equilibrated with 15–30 ml desalting buffer (A4) at a flow rate of 1 ml/min, and the 100 kD His-tagged protein was injected from AVR7-3 injection valve 2 (Figure 1). The His-tagged protein, salt, and imidazole were eluted until the UV and conductivity traces reached their baselines. During elution, the desalted 100 kD His-tagged protein was redirected to AVR7-3 sample loop 3 (Figure 1). Finally, the column was reequilibrated with 25 ml (2.5 CV) desalting buffer (A4).

Anion Exchange — The UNO Q1 anion exchange column was equilibrated with 10 ml (7.7 CV) ion exchange buffer A (A3) at a flow rate of 1 ml/min. The 100 kD His-tagged protein was injected from AVR7-3 injection valve 3 (Figure 1), and the column was washed with 10 ml (7.7 CV) ion exchange buffer A (A3) to remove unbound impurities. Next, the column was washed with 3 ml (2.3 CV) 10% ion exchange buffer B (B1) to remove weakly bound impurities. The 100 kD His-tagged protein was eluted from the column in 39 ml (30 CV) ion exchange buffer B (B1) at 10–60% strength. Finally, the column was washed with an additional 3 ml (2.3 CV) ion exchange buffer B (B1) at 100% strength to remove residual proteins from the column and then reequilibrated with 10 ml (7.7 CV) ion exchange buffer A (A3).

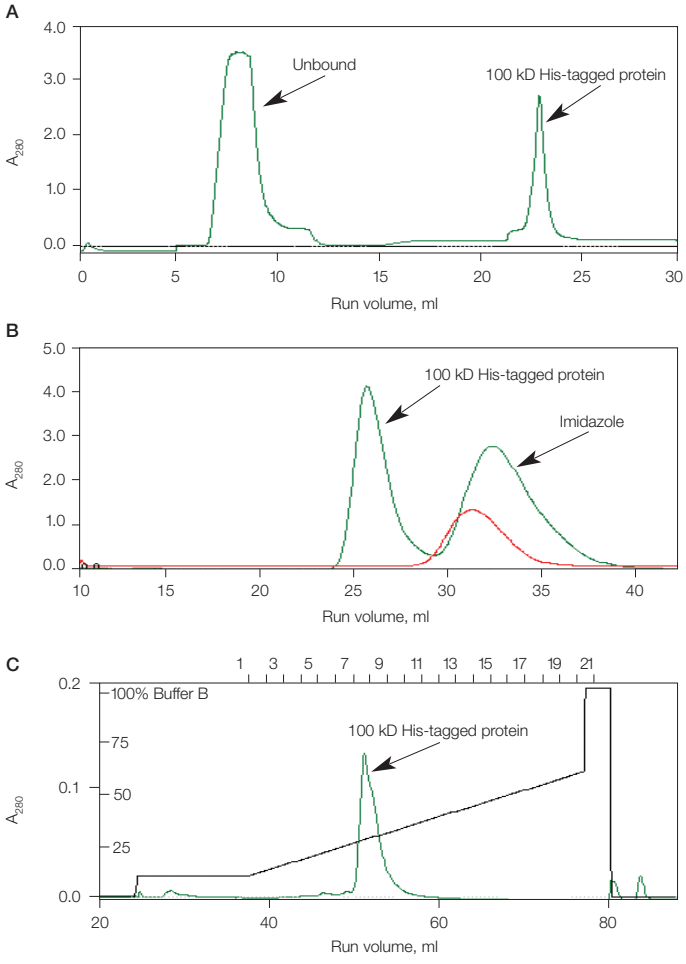

Fig. 2. Elution profiles of a 100 kD His-tagged protein purified from a crude *E. coli* lysate on the BioLogic DuoFlow Maximizer 20 chromatography system. Chromatograms plotted with BioLogic DuoFlow 5.1 software are shown following affinity capture on a Profinity IMAC column (**A**), desalting with Bio-Gel P-6DG desalting gel (**B**), and anion exchange on an UNO Q1 column (**C**).

Fraction Collection and Analysis

The elution profile during each step of the purification was monitored at 280 nm, and a series of 2 ml fractions was collected. Fractions containing the 100 kD His-tagged protein were analyzed by SDS-polyacrylamide gel electrophoresis (SDS-PAGE) on Criterion™ 4–20% gradient Tris-HCl polyacrylamide gels. Gels were analyzed using a GS-800™ densitometer and Quantity One® 1-D analysis software.

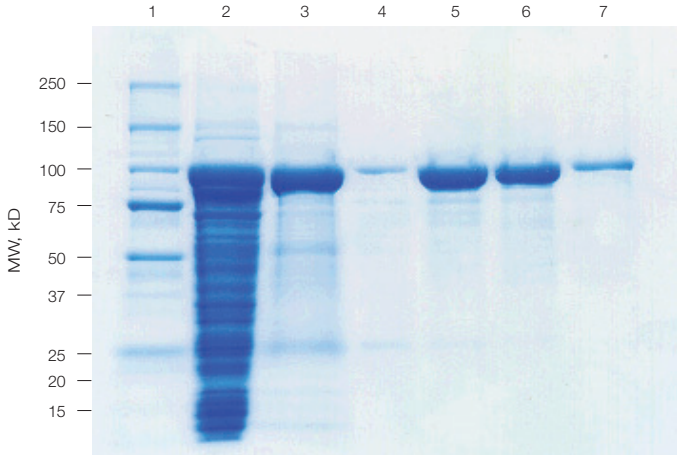

Fig. 3. SDS-PAGE analysis of fractions from three-dimensional purification of a 100 kD His-tagged protein. Lane 1, Precision Plus Protein™ standard; lane 2, crude *E. coli* lysate supernatant; lane 3, fraction eluted from the Profinity IMAC affinity column and containing the 100 kD His-tagged protein; lanes 4–7, four fractions containing 100 kD His-tagged protein eluted from the UNO Q1 anion exchange column.

Results

A crude *E. coli* lysate supernatant containing a 100 kD His-tagged protein of interest was loaded onto the BioLogic DuoFlow Maximizer 20 chromatography system configured as shown in Figure 1. The chromatograms obtained following affinity capture, desalting, and anion exchange were plotted by BioLogic DuoFlow 5.1 software and are shown in Figure 2.

SDS-PAGE analysis of the fractions containing the 100 kD His-tagged protein showed that the protein was substantially purified by this automated three-dimensional chromatographic process (Figure 3). Analysis of these gels revealed that the percent purity of the His-tagged protein following elution from the Profinity IMAC column was 78%, and that it reached 96% purity after anion exchange on the UNO Q1 column.

Conclusions

This study demonstrates that the BioLogic DuoFlow Maximizer 20 chromatography system, when used in combination with appropriate chromatographic media, is well suited to performing multidimensional chromatography. This automated system facilitates development of an efficient and robust protein purification process. Incorporating an automated multidimensional chromatographic process is especially advantageous for laboratories involved in structural or drug-target screening studies, where the automated purification of large amounts of pure and homogeneous protein can be a key factor in research success.

For additional copies of this article, request bulletin 5342.

New siLentMer™ siRNA!
Check out our new validated and nonvalidated 27-mer siRNA duplexes

Bio-Rad and RNAi. Come have a look.

From design to detection, Bio-Rad supports your RNAi research.

With a broad range of proven delivery technologies, award-winning detection systems, and a suite of high-quality support products, it's clear that Bio-Rad has a vision for RNAi.

- High-performing, potent siRNA for >85% knockdown with 5 nM or less siRNA
- Greatest choice of delivery technologies
- RNA and protein purification products
- Automated microfluidic RNA analysis
- Sensitive, optimized cDNA synthesis kits
- Systems for protein and mRNA detection

For a close look at Bio-Rad's tools for RNAi, visit us on the Web at **www.bio-rad.com/rnai/**

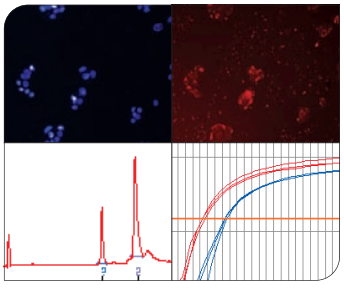

MCF-7 cells transfected using siLentFect™ reagent. RNA purified and analyzed using the Aurum™ total RNA kit and Experion™ system. Real-time PCR detection performed using iScript™ cDNA synthesis kit.

Visit us on the Web at **discover.bio-rad.com**
Call toll free at 1-800-4BIORAD (1-800-424-6723);
outside the US, contact your local sales office.

BIO-RAD

6X6

A Powerful Equation

The ProteOn™ XPR36 protein interaction array system, the ultimate in parallel processing.

Bio-Rad introduces the ProteOn XPR36, a surface plasmon resonance optical biosensor. Take the next step from protein discovery to function with label-free protein-protein interaction analysis. XPR™ technology is a unique 6 x 6 crisscross approach to multiplexing that processes, in parallel, 6 different ligands with 6 different analytes. Perform a complete kinetic analysis, rank a library of antibodies, or test multiple interaction conditions on a single chip, in a single run.

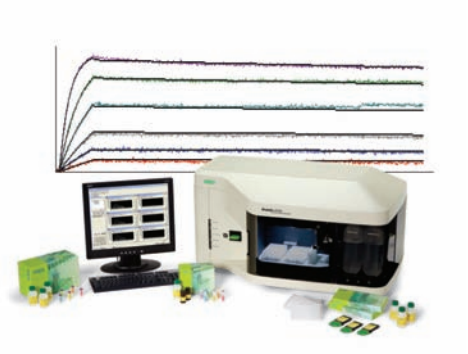

The 6 x 6 interaction array format provides:

- High-throughput parallel sample processing
- Full kinetic data
- Flexible experimental design

Visit us on the Web at **www.bio-rad.com/ad/proteininteraction/**

Visit us on the Web at **discover.bio-rad.com**
Call toll free at 1-800-4BIORAD (1-800-424-6723);
outside the US, contact your local sales office.

BIO-RAD